1973

The Spin-Up From Rest of a Homogeneous, Viscous Fluid in a Right Cylindrical Container.

William Benton Watkins
Louisiana State University and Agricultural & Mechanical College

The Spin-Up from Rest of a Homogeneous, Viscous Fluid in a Right Cylindrical Container

A Dissertation

Submitted to the Graduate Faculty of the
Louisiana State University and
Agricultural and Mechanical College
in partial fulfillment of the
requirements for the degree of
Doctor of Philosophy

in

The Department of Physics and Astronomy

by
William Benton Watkins
B.S., Louisiana State University, 1968
M.S., Louisiana State University, 1970
May, 1973

ACKNOWLEDGEMENTS

The author wishes to thank Professor R. G. Hussey for suggesting the problem and for his guidance and encouragement throughout this investigation. The author also wishes to thank Dr. Robert Williams and Mr. Burke Huner for many helpful discussions. The assistance of the Louisiana State University experimental physics technical staff, especially Mr. Lloyd Young, Mr. Leslie Edelen, Mr. Leo Jordan, Mr. Bob Sullivan, and Mr. Allen Young is gratefully acknowledged.

The calculations were done in cooperation with the Louisiana State University Computer Research Center, and their cooperation is greatly appreciated.

The author expresses gratitude to the National Science Foundation for financial assistance in the form of an NSF Traineeship. Portions of this work were supported by a National Science Foundation Research Grant.

The author would like to thank his wife and parents for their patience, love and unending encouragement.

TABLE OF CONTENTS

		Page
I.	INTRODUCTION	1
II.	THEORY	4
	A. The Wedemeyer Solution	4
	B. Broadening of the Velocity Front	6
	C. The Numerical Solution	7
	D. The Diffusion Solution	8
III.	EXPERIMENT	9
IV.	ANALYSIS AND RESULTS	14
	A. Dimensionless Time	14
	B. Comparison of Numerical and Experimental Times with Times Predicted by the Wedemeyer Theory	19
	C. Velocity Profiles	22
	1. Comparison of Wedemeyer profiles with numerical profiles	22
	2. Experimental profiles	24
	3. Axial independence of v in the interior flow region	27
	4. Comparison of Venezian profiles with numerical profiles	28
	D. Summary	37
APPENDIX I:	Tables of Data	40
	A. Experimental Data	40

Table of Contents (continued)

Page

B. Numerical Data and Computer Program. 45

APPENDIX II: Error Analysis 51

APPENDIX III: Electronics 54

REFERENCES 57

VITA 59

LIST OF TABLES

Table		Page
I.	The powers k, ℓ, m, and n for the dimensionless time T for the processes of convection and diffusion.	15
II.	Values of 0.01η and 0.1η for values of T and α_{min}	30
III.	Values of the lower bound of $\|\beta\|$ for various values of T.	34
IV.	Values of $\alpha_{min}\ \eta$ for values of α_{min} and T. . . .	35
V.	The range of times T over which Eqs. (26b) and (40b) both hold.	37

LIST OF FIGURES

Figure		Page
1.	Laser doppler velocimeter experimental setup; top view.	9a
2.	Laser doppler velocimeter experimental setup; side view.	9b
3.	An experimental spin-up curve.	11a
4.	The determination of radial position in the cylinder	12a
5.	Theoretical velocity profiles for spin-up mechanisms of diffusion and convection	14a
6.	The quantities k, 1-(ℓ/2), 2-2m and 2n obtained numerically as functions of ℓn α for W = 0.01, 0.1, 0.3, 0.5, 0.7 and 0.9	18a
7.	The quantities k, 1-(ℓ/2), 2-2m and 2n obtained both experimentally and numerically as functions of ℓn α for W = 0.5.	18b
8.	The ratios t_{Wed}/t_N and t_{Wed}/t_E as functions of the dimensionless parameter α.	20a
9.	Velocity profiles for the situation defined by h = 2.0 cm, a = 4.0 cm, ν = 0.01 cm^2/sec and Ω = 10.0/sec	22a
10.	Velocity profiles for the situation defined by h = 20.0 cm, a = 4.0 cm, ν = 0.01 cm^2/sec and Ω = 10.0/sec	22b

List of Figures (continued)

Figures		Page
11.	Velocity profiles for the situation defined by $h = 100.0$ cm, $a = 4.0$ cm, $\nu = 0.01$ cm^2/sec and $\Omega = 10.0$/sec	22c
12.	Experimental and numerical velocity profiles for $\alpha_{min} = 0.082$	26a
13.	Experimental and numerical velocity profiles for $\alpha_{min} = 0.217$	26b
14.	Experimental verification of the axial independence of v in the interior flow region	27a
15.	Active band pass filter circuit.	53
16.	a) Clipper circuit. b) Photomultiplier and preamplifier circuit	54

ABSTRACT

The spin-up from rest of a viscous, homogeneous fluid in a closed right circular cylinder is examined both experimentally and numerically. A laser doppler velocimeter is used to measure the azimuthal velocity component of the transient spin-up flow in the laboratory. A numerical integration of the Navier-Stokes equation is used to simulate spin-up from rest over wide ranges of cylinder dimensions, viscosities and speeds of rotation. The results are found to depend upon a dimensionless parameter $\alpha = h(\nu/\Omega)^{\frac{1}{2}}\left[r(a - r)\right]^{-1}$, where h is the height and a is the radius of the cylinder, r is the radial distance from the axis, ν is the fluid kinematic viscosity, and Ω is the angular speed of the cylinder. When α is small (<0.02) the convection model of Wedemeyer is valid; when α is not small, the effects of diffusion must be included. The parameter α is used to determine a more general form of the dimensionless time. The range of validity of a theory due to Venezian is examined in detail.

I. INTRODUCTION

Consider the problem of spin-up from rest of a homogeneous fluid of kinematic viscosity ν contained in a closed right circular cylinder of height h and radius a. Prior to some initial time t = 0 both the fluid and container are at rest. At time t = 0 the cylindrical container is impulsively spun about its axis from rest to some constant angular velocity Ω. A description of the transient fluid motion leading to rotation as a rigid body is required in terms of the quantities a, h, ν, and Ω.

By "spin-up" we mean the transient flow by which solid body rotation is achieved after an impulsive increase in angular speed of the container. Both convective and diffusive processes may be involved in this flow. Sometimes the term spin-up has been used to refer only to the convective process, but we prefer to use it in the more general sense stated above.

The spin-up from rest of a homogeneous fluid contained in a cylindrical container has been analyzed theoretically by Wedemeyer.[1] He considered the flow within the cylinder as occurring in two regions: (1) the boundary layers which are formed near the ends of the cylinder, and (2) the interior, i.e., everything outside the boundary layers. Side wall boundary layers were ignored. Neglecting the effects of viscosity in the interior and using a

momentum-integral approach for the flow at the ends, Wedemeyer obtained a single partial differential equation for the azimuthal velocity in the interior. The solution of this equation gives an advancing velocity front at which the radial derivative of the velocity is discontinuous. The solution accounts for the full nonlinearity of the problem, even though it involves approximations. Venezian[2,3] expanded on Wedemeyer's analysis and included several new features of the problem. His calculation of the structure of the velocity front predicted in Wedemeyer's article confirmed that the effects of viscosity erase the discontinuity.

Goller and Ranov[4] approached the spin-up from rest problem numerically. They calculated azimuthal velocities in the interior of an open-topped cylinder using a finite difference form of the Navier-Stokes equation which included the effects of both the deformation of the surface and radial outflow at the base. The deformation of the surface was also measured experimentally during various stages of the spin-up, and good agreement between calculations and experiment was obtained. It was concluded that the deformation of the surface tends to slow down the spin-up.

An experimental investigation of the spin-up from rest was reported by McLeod[5] in 1922. By timing the motion of lycopodium powder on the surface of an open rotating cylinder, McLeod was able to measure azimuthal velocities as a function of radial position and time. A wide range of experimental

conditions was used, and the infinite cylinder diffusion theory was presented for comparison with the measurements. Agreement was good only for the largest aspect ratio (h/a) cylinders rotating at the slowest speeds.

We report in this paper both experimental and numerical investigations of the spin-up from rest of a homogeneous fluid in a circular cylinder. Azimuthal velocities were measured with a laser doppler-velocimeter (LDV) operating in the reference beam mode. The numerical integration scheme of Goller and Ranov (without surface deformation) has been used to calculate the azimuthal velocity as a function of position and time over the following ranges of parameters: aspect ratio, $0.5 \leq h/a \leq 100$; Ekman number $1 \times 10^{-7} \leq \nu/(\Omega h^2) \leq 4 \times 10^{-3}$; and Reynolds number, $4 \times 10^2 \leq a^2\Omega/\nu \leq 1 \times 10^5$. The experimental ranges of these parameters were $1.06 \leq h/a \leq 9.02$; $3.06 \times 10^{-6} \leq \nu/\Omega h^2 \leq 3.42 \times 10^{-3}$; and $1.88 \times 10^3 \leq a^2\Omega/\nu \leq 2.52 \times 10^4$. The results of the measurements and calculations are compared with Wedemeyer's theory and Venezian's expression for the broadening of the velocity front. A non-dimensional parameter $\alpha\{ = h(\nu/\Omega)^{\frac{1}{2}}[r(a-r)]^{-1}$, where r is the radial position} has been found which expresses the relative importance of convection and diffusion in spin-up from rest. When α is small, convection dominates and the Wedemeyer theory applies; at larger values of α, the effects of diffusion must be included.

II. THEORY

A. The Wedemeyer Solution

In an inertial cylindrical coordinate system (r,θ,z) with origin at the center of the cylinder, the Navier-Stokes equations for velocity components (u,v,w) are

$$\frac{\partial u}{\partial t} + u\frac{\partial u}{\partial r} + w\frac{\partial u}{\partial z} - \frac{v^2}{r} = -\frac{1}{\rho}\frac{\partial p}{\partial r} + \nu\left(\nabla^2 u - \frac{u}{r^2}\right) \tag{1}$$

$$\frac{\partial v}{\partial t} + u\left(\frac{\partial v}{\partial r} + \frac{v}{r}\right) + w\frac{\partial v}{\partial z} = \nu\left(\nabla^2 v - \frac{v}{r^2}\right) \tag{2}$$

$$\frac{\partial w}{\partial t} + u\frac{\partial w}{\partial r} + w\frac{\partial w}{\partial z} = -\frac{\partial p}{\partial z} + \nu\nabla^2 z \tag{3}$$

where $\nabla^2 = \frac{\partial^2}{\partial r^2} + \frac{1}{r}\frac{\partial}{\partial r} + \frac{\partial^2}{\partial z^2}$

where rotational symmetry has been assumed. It is convenient to consider the flow within the cylinder as occurring in (1) the boundary layers, and (2) the interior, where the radial and axial velocities u and w will be much smaller than the azimuthal velocity v. In the interior, therefore, Eqs. (1)-(3) can be approximated by

$$\frac{v^2}{r} = \frac{1}{\rho}\frac{\partial p}{\partial r} \tag{1a}$$

$$\frac{\partial v}{\partial t} + u\left(\frac{\partial v}{\partial r} + \frac{v}{r}\right) + w\frac{\partial v}{\partial z} = \nu\left(\nabla^2 v - \frac{v}{r^2}\right) \tag{2a}$$

$$0 = \frac{\partial p}{\partial z}\,. \tag{3a}$$

From (3a) we see that the pressure is nearly independent

of z. Then, from (1a), v must be independent of z also, and from (2a), so must u. The resulting form of (2a) is

$$\frac{\partial v}{\partial t} + u\left(\frac{\partial v}{\partial r} + \frac{v}{r}\right) = \nu\left(\frac{\partial^2 v}{\partial r^2} + \frac{\partial}{\partial r}\left(\frac{v}{r}\right)\right). \tag{4}$$

Equation (4) was obtained by Wedemeyer.[1] By considering that the boundary layer flow is essentially steady, Wedemeyer obtained a relation between u and v of the form[6]

$$u = -E^{\frac{1}{2}}(r\Omega - v) \tag{5}$$

where E is the Ekman number, $\nu/\Omega h^2$. Then Eq. (4) for v becomes

$$\frac{\partial v}{\partial t} - E^{\frac{1}{2}}(r\Omega - v)\left(\frac{\partial v}{\partial r} + \frac{v}{r}\right) = \nu\left(\frac{\partial^2 v}{\partial r^2} + \frac{\partial}{\partial r}\left(\frac{v}{r}\right)\right). \tag{6}$$

Introducing the dimensionless variables $V = v/a\Omega$, $R = r/a$, and $T = E^{\frac{1}{2}}\Omega t$, we can rewrite Eq. (6) in dimensionless form

$$\frac{\partial V}{\partial T} - (R - V)\left(\frac{\partial V}{\partial R} + \frac{V}{R}\right) = \left(\frac{h}{a}\right)^2 E^{\frac{1}{2}}\left[\frac{\partial^2 V}{\partial R^2} + \frac{\partial}{\partial R}\left(\frac{V}{R}\right)\right]. \tag{7}$$

When the quantity $(h/a)^2E^{\frac{1}{2}}$ is sufficiently small, the right hand side of (7) may be neglected. The resulting equation was solved by Wedemeyer; the solution is

$$\begin{aligned} V &= (Re^{2T} - R^{-1})/(e^{2T} - 1), \quad R \geq e^{-T} \\ V &= 0 \qquad\qquad\qquad\qquad\quad , \quad R \leq e^{-T}. \end{aligned} \tag{8}$$

Equation (8) predicts the existence of a velocity front which originates at the container wall (R=1) and moves inward with time, separating rotating fluid behind the front ($R>e^{-T}$)

from quiescent fluid ahead of the front ($R<e^{-T}$). Wedemeyer predicted that the effect of viscosity should broaden this front so that the velocity derivative would change continuously from $R>e^{-T}$ to $R<e^{-T}$.

The physical interpretation of the convection process is quite simple. The viscous boundary layers (Ekman layers) formed on the ends of the container are established in a time $2/\Omega$, and are essentially steady thereafter. Fluid in these layers is transported radially outward by the centrifugal force and is given angular momentum in the process. This fluid which has acquired angular momentum is forced into the interior behind the velocity front by the container walls. By conservation of mass, fluid must be drawn axially into the boundary layers, and in the case of spin-up from rest, all of the fluid in the container must be circulated in this way for the spin-up to be completed. The convective process is accomplished in a time of order $E^{-\frac{1}{2}}\Omega^{-1}$. Boundary layers at the side walls of the container are assumed to play a passive role.

B. Broadening of the Velocity Front

From physical considerations one may argue that the velocities and derivatives of the flow ahead of the front should join to the velocities and derivatives of the flow behind the front in a continuous manner. Venezian[3] has calculated the structure of the front using the complete

Eq. (6). The solution is given in terms of the complementary error function erfc(x) and the variables $\xi = R^2 e^{2T}$, $\eta = e^{2T}-1$:

$$V = \frac{4hE^{\frac{1}{4}} e^{-\zeta^2/2\eta}}{r(2\pi\eta)^{\frac{1}{2}} \operatorname{erfc}(\zeta/\sqrt{2\eta})} \qquad (9)$$

where ζ is defined by $\xi = (1 + \frac{2hE^{\frac{1}{4}}}{a}\zeta)$ and r is the radial coordinate. The position of the velocity front in terms of these variables is $\xi = 1$. The front is a layer of width proportional to $E^{\frac{1}{4}}$, and is similar in nature to the $E^{\frac{1}{4}}$ and $E^{1/3}$ layers investigated by Stewartson.[7] Basically the $E^{\frac{1}{4}}$ layer provides a continuous change in azimuthal velocity and derivatives in the region of the front, and the $E^{1/3}$ layer, which presumably remains attached to the container wall, provides a continuous change of the axial velocities and derivatives at the wall.

C. The Numerical Solution

Goller and Ranov[4] developed a numerical integration of Eq. (4) to calculate azimuthal velocities and surface profiles for their experiment. By considering the flow in a closed cylinder to be symmetric about the cylinder's mid-plane, and by omitting the terms for surface deformation, we have adapted their method to the problem considered in this paper. In this method the radial velocity u is related to the azimuthal velocity v through a 7th order polynomial fit to the points given by Rogers and Lance.[8] A nested form of the polynomial is:

$$U = .442230+(.536161)W\left[1-8.80327W(1-2.528307W(1-1.609258W(1-0.993635W(1-0.550504W(1-0.231796W))))\right]. \qquad (9)$$

where $U = uh(\nu\Omega)^{-\frac{1}{2}}/r$ and $W = v/r\Omega$.

D. The Diffusion Solution

If the aspect ratio h/a is very large or if the fluid is very viscous, one would expect diffusion of momentum from the side wall to play a larger role in spin-up. It is well known[9] that the nondimensional time appropriate to the diffusion of momentum over a distance L is $T_d = \frac{L^2}{\nu}t$. With this time scale and with the dimensionless variables $T_d = ta^2/\nu$, $U = u/a\Omega E^{\frac{1}{2}}$, $V = v/a\Omega$, $R = r/a$, Eq. (4) becomes

$$\frac{\partial V}{\partial T_d} + \left(\frac{a}{h}\right)^2 E^{-\frac{1}{2}} U\left(\frac{\partial V}{\partial R} + \frac{V}{R}\right) = \left(\frac{\partial^2 V}{\partial R^2} + \frac{\partial}{\partial R}\left(\frac{V}{R}\right)\right). \qquad (10)$$

When the coefficient of the second term on the left hand side of (10) is small, the diffusion equation results. The solution is well-known:

$$V = R + 2\Sigma \frac{J_1(\lambda_n R)}{\lambda_n J_o(\lambda_n)} \exp\left(-\lambda_n^2 \frac{\nu t}{a^2}\right) \qquad (11)$$

where J_1 (J_o) is the Bessel function of the first kind of order one(zero) and λ_n satisfies $J_1(\lambda_n) = 0$, $\lambda_n > 0$. It should be pointed out that the choice of variables used to make the radial velocity dimensionless implies that the Ekman layer thickness $(\nu/\Omega)^{\frac{1}{2}}$ is small compared to the fluid depth h.

III. EXPERIMENT

The experimental arrangement is shown in Figs. 1 and 2. The azimuthal velocity in the interior of the cylinder has been measured experimentally using a laser doppler velocimeter (LDV) operating in the reference beam mode.[10] A low power (~1.5mw) He-Ne laser was aimed at an uncoated optical flat which served as beam splitter.[11] The transmitted and internally reflected portions of the beam were of suitable intensities for use as scattering and reference radiation, respectively. A 175mm focal length lens focused both beams at their point of intersection in the test section.

The cylinders used were machined from Plexiglas tubing to be round and concentric to less than .05mm, and then were hand polished using successively finer grades of lens grinding abrasives. The base of the cylinder in use was screw mounted to a turntable which was enclosed in a Plexiglas box. The turntable shaft was made from 1.27 cm diameter centerless ground stainless steel rod. The shaft was supported by a bearing below the Plexiglas box, and sealed by an O-ring as it passed through the bottom of the box. By filling the space between the box and the cylinder with a fluid medium (Dow Corning 710 Silicone Fluid) of refractive index very nearly the same as that of Plexiglas, distortions were virtually eliminated, and the only optical density change undergone by the laser beam once inside the box was

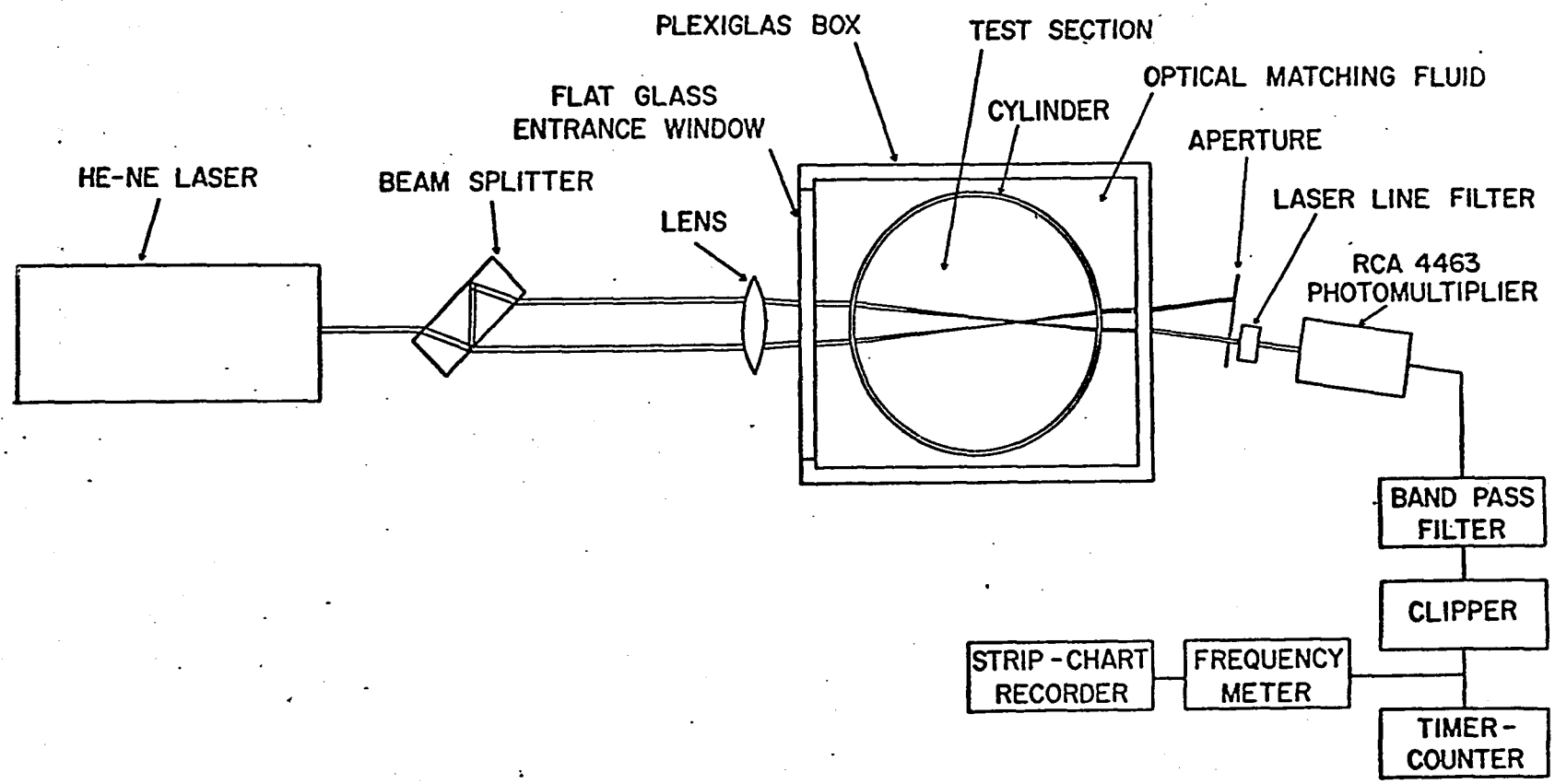
PLEXIGLAS BOX
TEST SECTION
OPTICAL MATCHING FLUID
FLAT GLASS
ENTRANCE WINDOW
CYLINDER
APERTURE
HE-NE LASER
BEAM SPLITTER
LENS
LASER LINE FILTER
RCA 4463
PHOTOMULTIPLIER
BAND PASS
FILTER
CLIPPER
STRIP-CHART
RECORDER
FREQUENCY
METER
TIMER-
COUNTER

Fig. 1

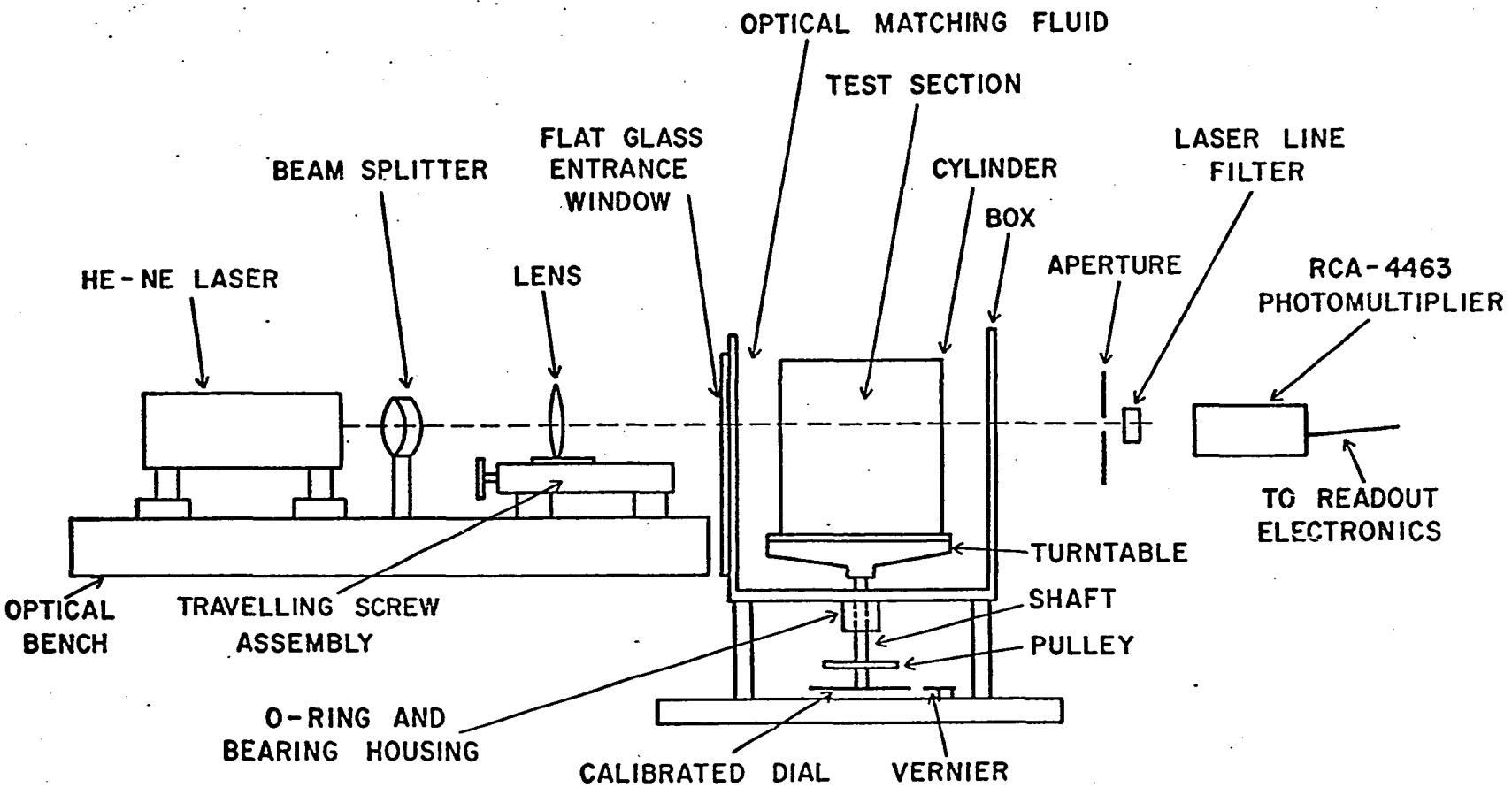
OPTICAL MATCHING FLUID
TEST SECTION
FLAT GLASS ENTRANCE WINDOW
BEAM SPLITTER
CYLINDER
LASER LINE FILTER
BOX
APERTURE
HE-NE LASER
LENS
RCA-4463 PHOTOMULTIPLIER
TO READOUT ELECTRONICS
TURNTABLE
SHAFT
PULLEY
OPTICAL BENCH
TRAVELLING SCREW ASSEMBLY
O-RING AND BEARING HOUSING
CALIBRATED DIAL
VERNIER

Fig. 2

as it encountered the column of test fluid inside the cylinder. A flat glass plate was used as an entrance window in one face of the box to avoid misalignment of the beams by local prismatic refraction.

The cylinders were rotated with a belt pulley system driven by a Graham BD4MW60 transmission. The pulleys employed provided a range of angular speed Ω from 0.52 to 4.15 rad/sec. Four different diameter cylinders were used: 14.72 cm, 13.92 cm, 9.03 cm, and 8.86 cm. The first two were of heights equal to the diameter. The two smaller diameter cylinders were used with pistons which were machined to the inner diameters of the cylinders so that the effect of changing the height of the column of fluid on the spin-up could be noted. Heights ranging from 39.90 to 4.52 cm were obtained with these two cylinders. The fluids used were distilled water and solutions of sucrose in water. Viscosities of the sucrose solutions were measured using Cannon-Fenske viscometers immersed in a constant temperature bath. The viscosity of water was determined as a function of temperature from tables.[12] A range of viscosities from .0088 to .034 cm^2/sec was obtained with these working fluids.

The mixed signal and reference radiation passed through an aperture and laser line filter to an RCA 4463 (S-20 response) photomultiplier. An active band pass filter[13] of half power points 0.8 and 50 kHz fed the signal to an amplifier, after which it was clipped to ±0.3v amplitude by a diode shunt limiter, and then analyzed by a Hewlett Packard 5210A frequency meter and 5362B timer counter. The analog voltage from the frequency meter was recorded by a Moseley 7101B strip chart recorder and the digital readings were recorded by hand on the chart opposite event markers provided by the timer-counter. A remote switch allowed the motor driving the transmission and turntable to be started as the recorder pen crossed one of the major divisions of the chart. The strip chart rate was used as the timer for the experiments. This rate was found to be accurate to within a few seconds over a period of an hour. Curves similar to the one shown in Fig. 3 were obtained. Both noise and the event markers have been omitted for clarity.

The observed frequency shift f_D is given by

$$f_D = \frac{1}{2\pi}(\vec{k}_s - \vec{k}_i)\cdot\vec{v} \qquad (12)$$

where $\vec{v}$ is the flow velocity and $\vec{k}_s$ and $\vec{k}_i$ are the wavevectors of the scattered and incident beams, respectively. The measured component of $\vec{v}$ is known to be in the azimuthal direction. It can be shown that (see Fig. 4)

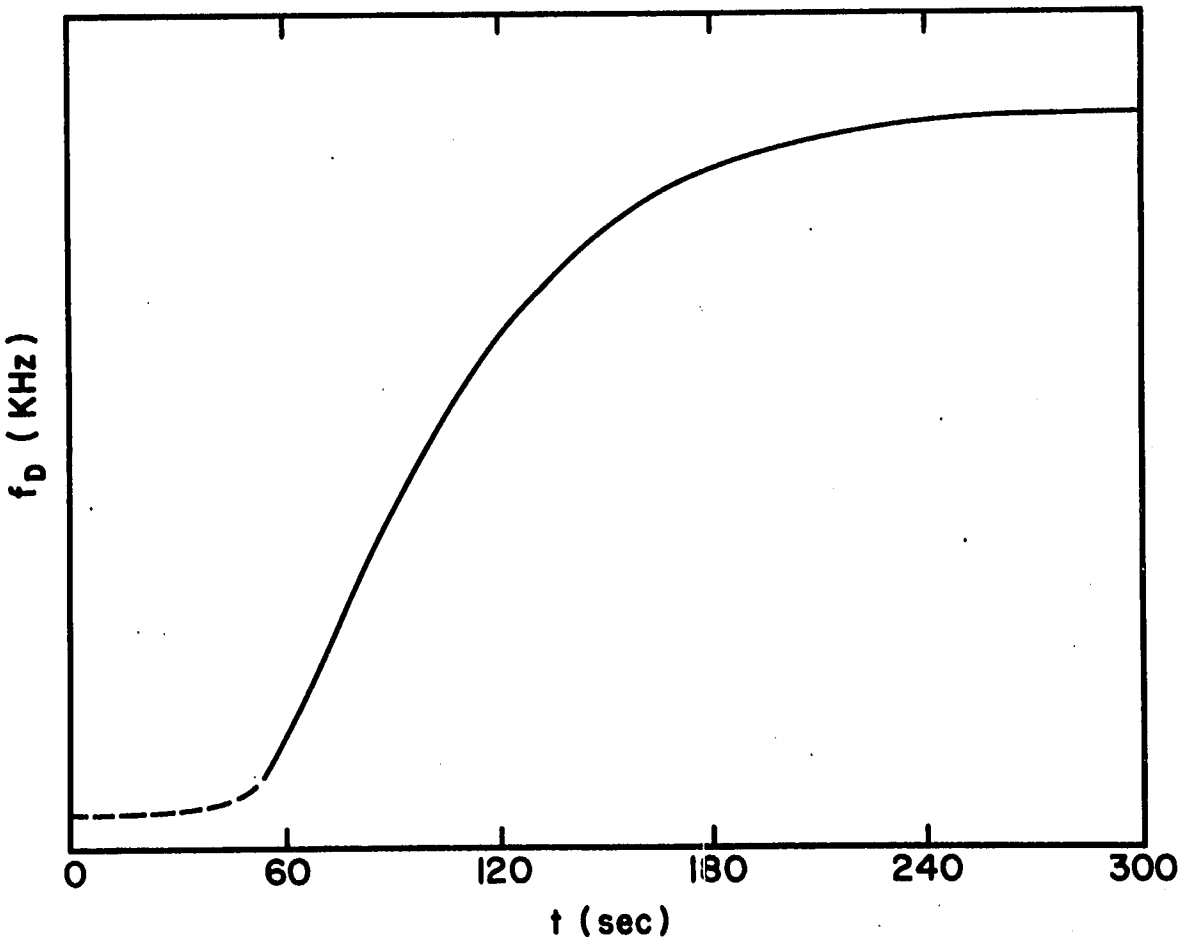

Fig. 3

$$f_D = \left[\frac{2n}{\lambda_o}\sin\theta\right] v \qquad (13)$$

where n is the index of refraction of the test medium, λ_o is the wavelength of the laser light in air, and 2θ is the angle of intersection of the two beams.

The radial position r at which the beams intersected was determined as follows: An engraved disc dial was attached to the turntable shaft outside the Plexiglas box, and angular readings were made using a vernier which was fixed relative to the dial. A thin glass fiber was taped to the cylinder wall inside the cylinder. The turntable was rotated by hand until the fiber marked the position of the center of one of the beams. The reading of the dial-vernier was then recorded, and the procedure was repeated for each of the three other beams. Differences in angular position readings yielded the angles ϕ_1 and ϕ_2 defined in Fig. 4 . The radial position r of the test point was determined by application of the law of sines to triangles ABC and BCD of Fig. 4 . An expression for r is

$$r = \frac{a}{2} \frac{\sin\left(\frac{\phi_1 - \phi_2}{2}\right)}{\sin\left(\frac{\phi_1 + \phi_2}{4}\right) \cos\left(\frac{\phi_1 - \phi_2}{4}\right)} \; . \qquad (14)$$

The least count of the dial-vernier was six minutes of arc, and the corresponding accuracy in radial position $\frac{\Delta r}{r}$ was 5%.

The doppler frequency shift was calculated using Eq. (13) where θ is defined by $\theta = \tan^{-1}\left[\frac{s}{2(a+r)}\right]$ and $s = 2a\sin\left(\frac{\phi_1}{2}\right)$.

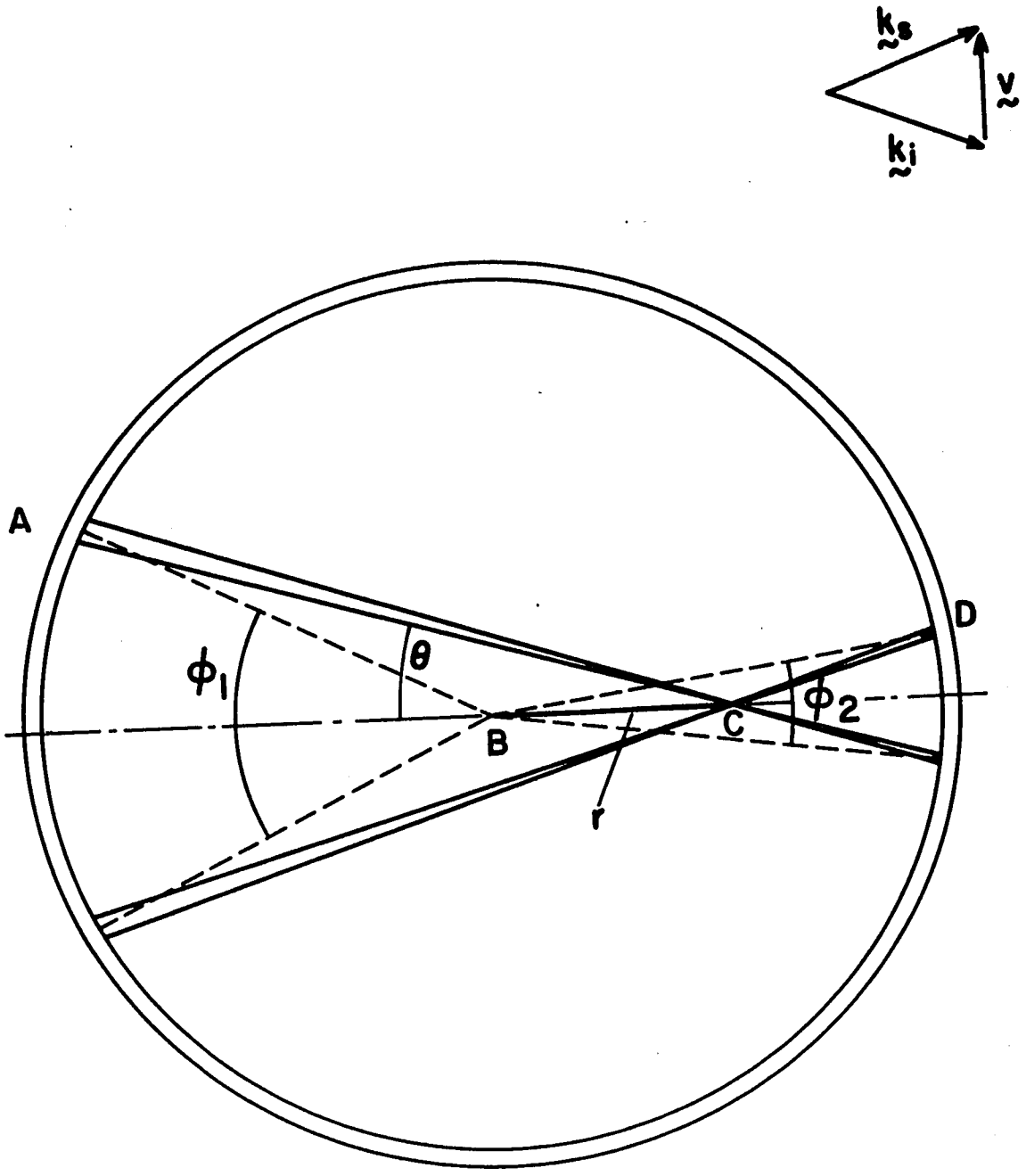
$\underset{\sim}{k_s}$
$\underset{\sim}{v}$
$\underset{\sim}{k_i}$
A
D
ϕ_1
θ
ϕ_2
B
C
r

Fig. 4

The frequency calculated for solid body rotation in this manner usually agreed with that measured to within 5%. A further discussion of errors is contained in Appendix II.

IV. ANALYSIS AND RESULTS

A. Dimensionless Time

Two approximate solutions to the problem of spin up from rest were presented in Section II. In the first solution (Eq. (8)), due to Wedemeyer, the mechanism for spin-up is the convective circulation established by the Ekman layers at the ends of the container. One expects this solution to be valid when the coefficient $\frac{h}{a^2}(\frac{\nu}{\Omega})^{\frac{1}{2}}$ of the right hand side of Eq. (7) is small. The time scale for the convective process is $h(\nu\Omega)^{-\frac{1}{2}}$. In the second solution (Eq. (11)), the mechanism for spin-up is viscous diffusion from the side walls of the container. One expects this solution to be valid when the coefficient $\frac{a^2}{h}(\frac{\Omega}{\nu})^{\frac{1}{2}}$ of the second term of the left hand side of Eq. (10) is small. The time scale for the diffusive process is a^2/ν. The parameter $\frac{h}{a^2}(\frac{\nu}{\Omega})^{\frac{1}{2}}$ is recognized as the ratio of the convective time scale to the diffusive time scale. The two solutions are shown in Fig. 5, in which the dimensionless angular velocity $W = v/r\Omega$ is presented as a function of the dimensionless radial position $R = r/a$. The solid lines obtained from Eq. (8) are velocities at constant values of the dimensionless time $T_c = t(\nu\Omega)^{\frac{1}{2}}h^{-1}$. The dashed lines obtained from Eq. (11) are velocities at constant values of the dimensionless time $T_d = \nu a^{-2}t$. For each set of velocity

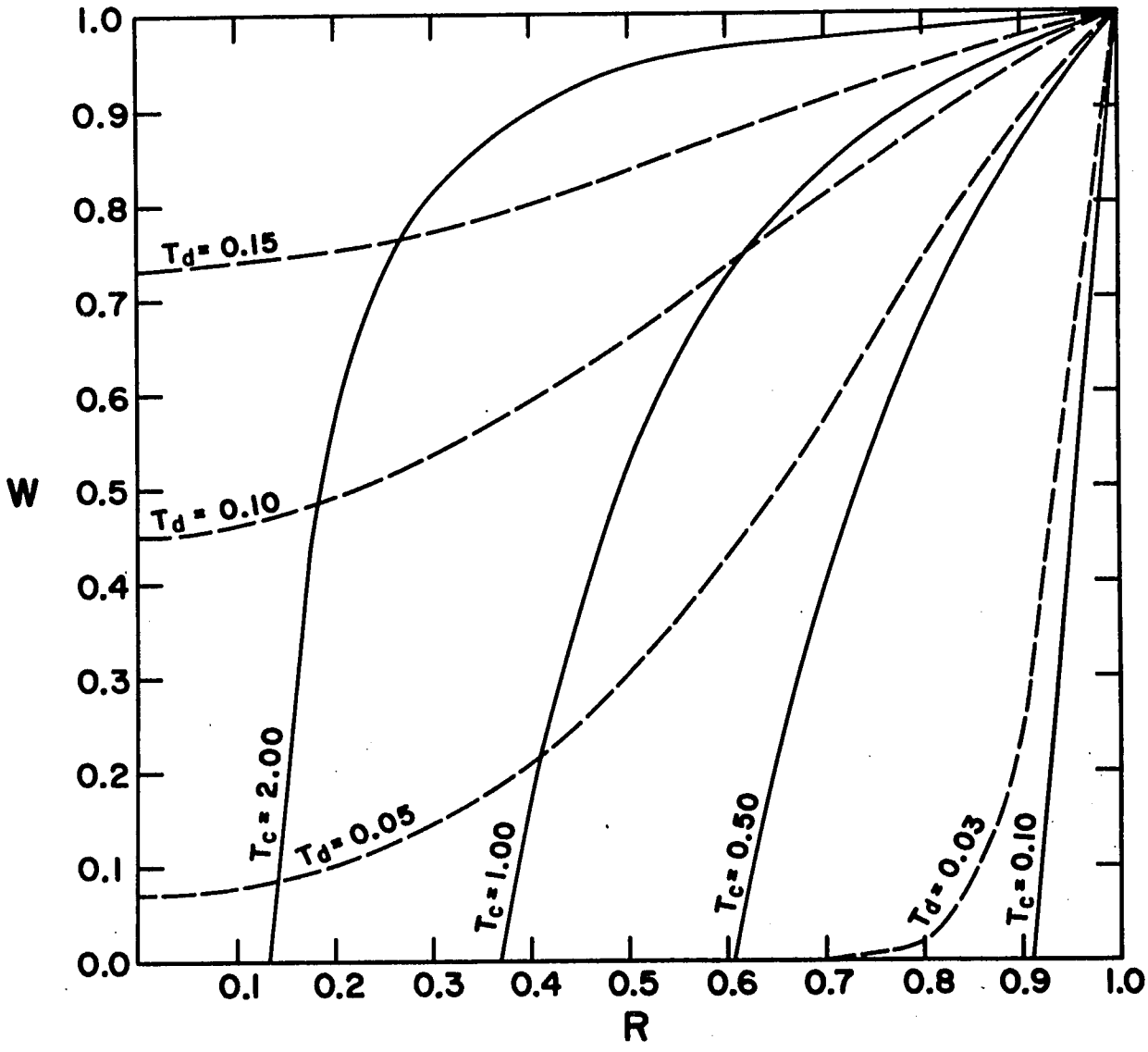
1.0
0.9
0.8
0.7
0.6
0.5
0.4
0.3
0.2
0.1
0.0
W
0.1
0.2
0.3
0.4
0.5
0.6
0.7
0.8
0.9
1.0
R
Td = 0.15
Td = 0.10
Td = 0.05
Tc = 2.00
Tc = 1.00
Tc = 0.50
Td = 0.03
Tc = 0.10

Fig. 5

profiles, the form of the dimensionless time is independent of both radial position and the value of W.

We have investigated the dimensionless time both experimentally and numerically. The results are: (1) the dimensionless time must be expressed in a more general form, of which T_c and T_d are special cases; (2) the expression for the dimensionless time depends not only on the value of the parameter $(\frac{h}{a^2})(\frac{\nu}{\Omega})^{\frac{1}{2}}$ but also on the radial position R; and (3) the expression for the dimensionless time depends on the value of W.

A general form of the dimensionless time T which includes both T_c and T_d is:

$$T = \frac{\nu^m \Omega^n}{h^k a^\ell} t. \tag{15}$$

The powers k, ℓ, m, and n which are appropriate to the spin up mechanisms of convection and diffusion are summarized in Table I.

Table I

Process	k	ℓ	m	n
Convection	1	0	0.5	0.5
Diffusion	0	2	1	0

If T is to be dimensionless, then k, ℓ, m, and n must satisfy the dimensional constraints

$$m + n = 1 \tag{16a}$$

$$k + \ell = 2m \tag{16b}$$

The investigation of the dimensionless time T was undertaken in the following manner. A given parameter was chosen from the set $\{a,h,\nu,\Omega\}$. For purposes of illustration let this parameter be Ω. The value of Ω was chosen to be Ω_1 in the first set of calculations (experiments) and t_1 was found to be the time required for the dimensionless angular velocity W to become a certain value (e.g., 0.5) at a fixed R. The value of Ω was changed to Ω_2 in the second set of calculations (experiments) and t_2 was found to be the time required for W to become the specified value at the same R, with other conditions unchanged. The power law which describes the effect of Ω on the rate at which spin up proceeds is

$$\frac{t_1}{t_2} = \left(\frac{\Omega_1}{\Omega_2}\right)^n \tag{17a}$$

or

$$n = \frac{\ell n(t_1/t_2)}{\ell n(\Omega_1/\Omega_2)} \, . \tag{17b}$$

Changes in a, h, ν, and Ω were done numerically. Changes in Ω and h were done experimentally.

The powers k, ℓ, m, and n were found to be functions of both an empirical parameter

$$\alpha = (h/a)^2 E^{1/2}/[R(1-R)] = [(\nu/\Omega)^{1/2} h/a^2]/[R(1-R)] \qquad (18)$$

and the dimensionless angular velocity W. Each power was determined by the method of Eqs. (17) as a function of the midpoint of the interval α_1 to α_2. In the example of the previous paragraph, $\alpha_1 = \alpha_1(\Omega_1,a,h,\nu,R)$ and $\alpha_2 = \alpha_2(\Omega_2,a,h,\nu,R)$.

The initial efforts to determine the powers k, ℓ, m, and n were directed to the set of numerical data for which W = 0.5. It was found that when the powers were plotted as functions of the dimensionless parameter α, each plot was a smooth, monotonic curve. The limiting values of the powers for $\alpha \to 0$ (convection) and $\alpha >> 1$ (diffusion) were found to be the powers given in Table I. The dimensional constraints (16a) and (16b) were verified from (and not imposed on) these plots.

It was found from the plots of the powers as functions of α that a third relation holds:

$$k + 2m = 2. \qquad (16c)$$

This relation proved to be valid over the entire range of α investigated. The relations (16a), (16b), and (16c) may be used to determine one power in terms of any one of the other three. The power k proved to be a convenient choice:

$$k = 2n = 1 - (\ell/2) = 2 - 2m. \qquad (19)$$

If the relations of Eq. (19) are employed, then the quantities k, 2n, 1 - (ℓ/2) and 2 - 2m may be plotted as functions of α to determine a single curve. This is shown in Fig. 6. All of the points in Fig. 6 were obtained from the numerical solution of Eq. (4). The different symbols refer to the different quantities in Eq. (19). The scatter in these points is due to the finite difference method used to determine the powers. The fact that the powers k, ℓ, m, and n, determined independently, result in a single curve when plotted as in Fig. 6 , gives us confidence that α is the correct parameter for determining the form of the dimensionless time.

Dimensionless times for levels of rotation other than W = 0.5 were also investigated and the results are shown in Fig. 6. Again, the same relations between the powers (Eq. (19)) were found to hold, and the same limiting values (Table I) were obtained for extremes of α. However, for intermediate values of α ($0.05 < \alpha < 5$), the curves were found to depend upon the value of W. As W decreases, the form of the dimensionless time becomes more "diffusion-like". This is not surprising, since the velocity front occurs at small values of W, and diffusion is expected to play a larger role in spin up near the velocity front.

The numerical curve for W = 0.5 is compared with experiment in Fig. 7 . The experimental points are taken

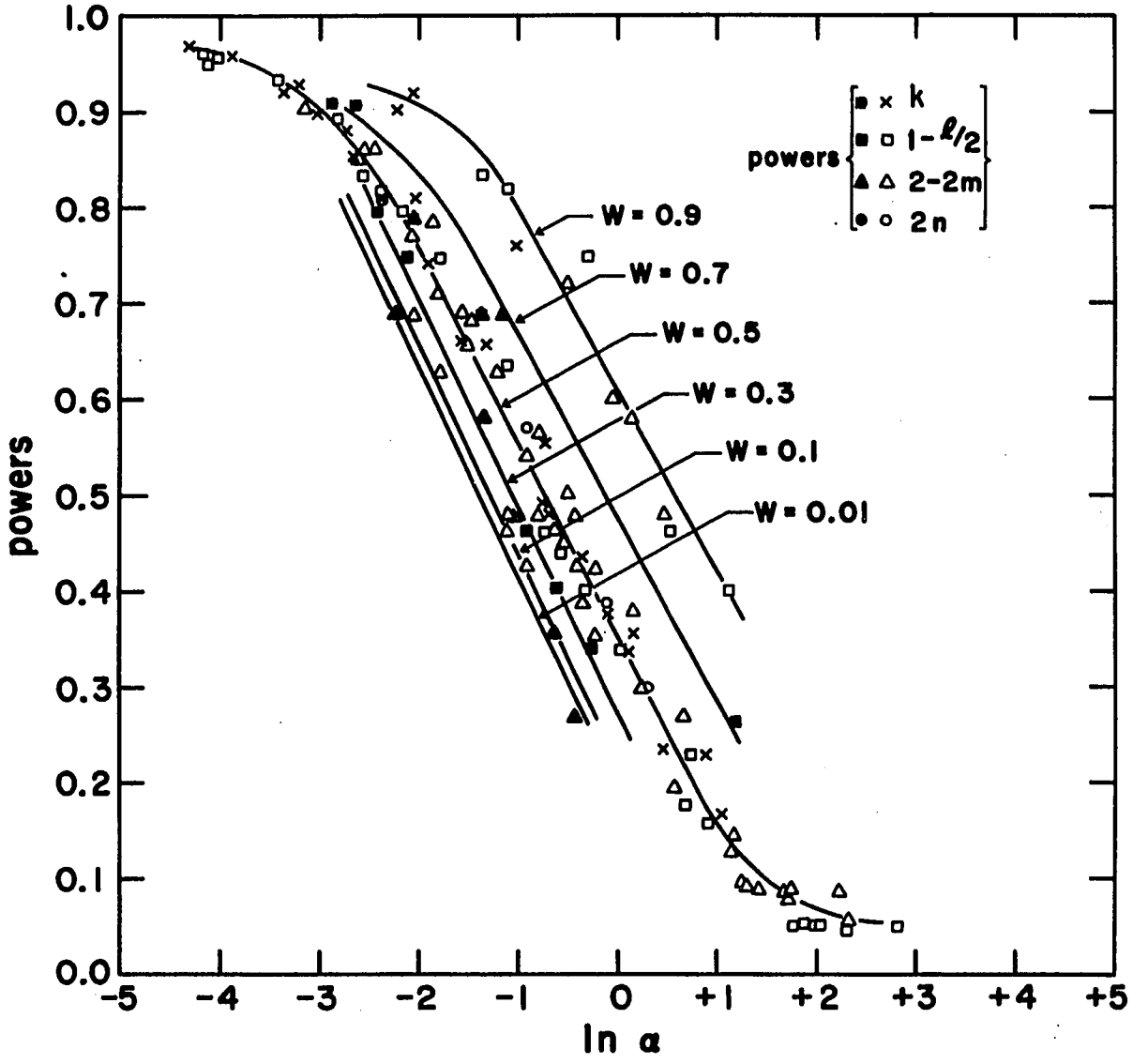
1.0
0.9
0.8
0.7
0.6
0.5
0.4
0.3
0.2
0.1
0.0
powers
-5
-4
-3
-2
-1
0
+1
+2
+3
+4
+5
ln α
W = 0.9
W = 0.7
W = 0.5
W = 0.3
W = 0.1
W = 0.01
powers
× k
□ 1-ℓ/2
△ 2-2m
○ 2n

Fig. 6

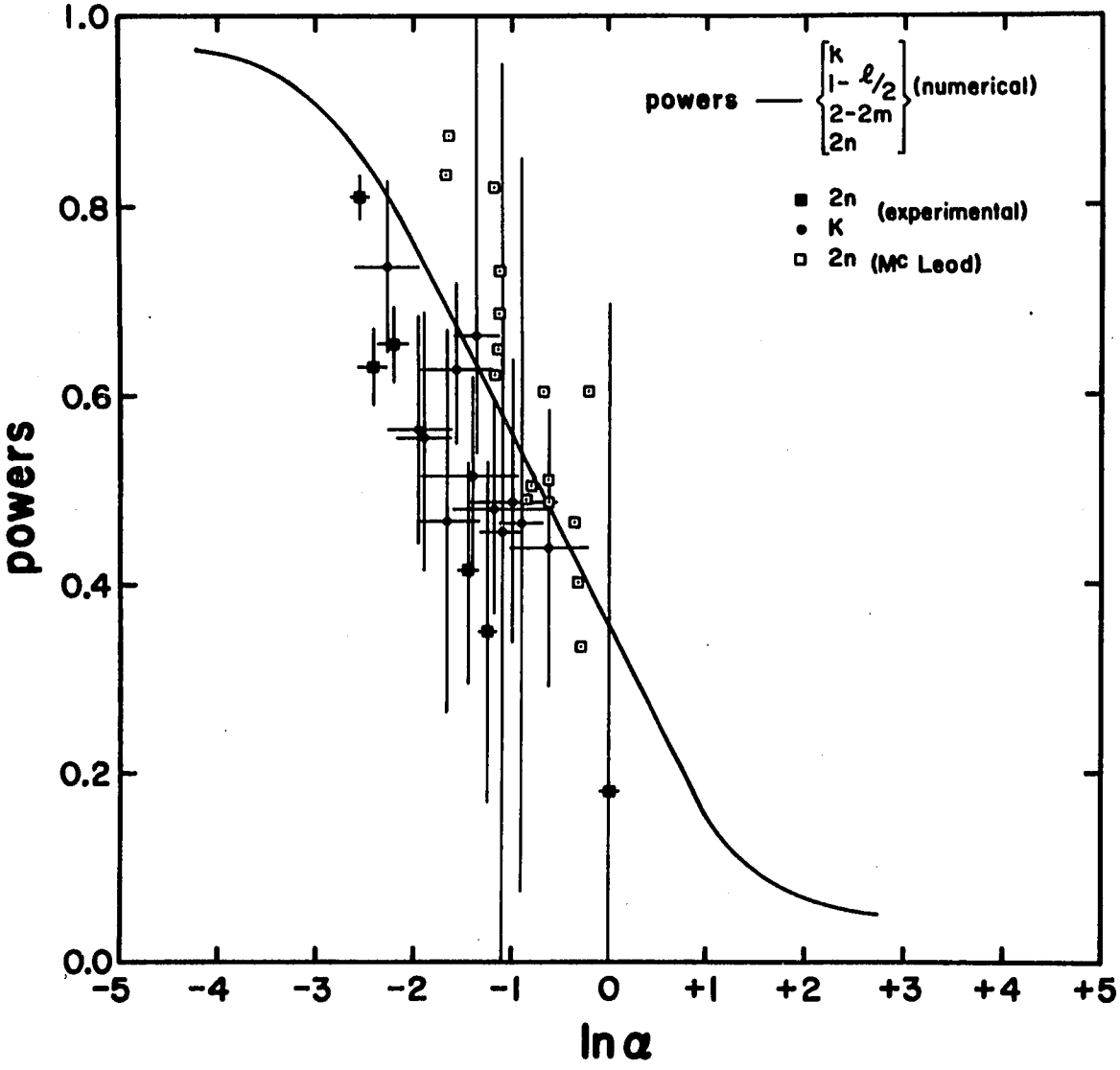
1.0
0.8
0.6
0.4
0.2
0.0
powers
-5
-4
-3
-2
-1
0
+1
+2
+3
+4
+5
ln α
powers — {k, l- ℓ/2, 2-2m, 2n} (numerical)
2n (experimental)
K
2n (Mc Leod)

Fig. 7

from the present work and also from the curves given by McLeod. The errors in the experimental points are large due to the fact that the finite difference method of obtaining the powers magnifies errors in the experimental quantities. The points from the present work tend to be lower than the numerical curve and the points from McLeod's work tend to be higher than the numerical curve. However, both experiments confirm the general conclusion of the numerical studies, namely that the form of the dimensionless time changes smoothly from "convection-like" for $\alpha << 1$ to "diffusion-like" for $\alpha > 1$.

B. Comparison of Numerical and Experimental Times with Times Predicted by the Wedemeyer Theory

The numerical times t_N and the experimental times t_E for the velocity at a fixed position to reach a given fraction of sold-body rotation were compared with the corresponding times t_{Wed} predicted by the Wedemeyer theory. The times t_{Wed} were obtained by solving Eq. (8). For example, if W = 0.5, then

$$t_{Wed} = \frac{h}{2\sqrt{\nu\Omega}} \ln\left(\frac{2}{R^2} - 1\right). \qquad (20)$$

It was found that for a given value of W the time t_{Wed} obtained in this manner was always larger than both the experimentally observed time t_E and the numerically obtained

time t_N. The ratios t_{Wed}/t_E and t_{Wed}/t_N were found to depend on the value of W and on the value of the dimensionless parameter α. These results are shown in Fig. 8 . It is apparent that in the limit $\alpha \to 0$, the Wedemeyer expression (Eq. (8)) accurately predicts the times for different values of the dimensionless angular velocity W to occur. The times t_{Wed} predicted by Eq. (8) for values of $W \geq 0.5$ are accurate to within 20% for $\alpha \leq 0.03$. The times t_{Wed} predicted by Eq. (8) for $W = 0.3$ are accurate to within 20% for $\alpha \leq 0.01$.

Inspection of both the expression for α

$$\alpha = (\frac{h}{a})^2 E^{\frac{1}{2}} / [R(1 - R)] \qquad (21)$$

and Fig. 8 reveals immediately that either large values of the aspect ratio h/a or extreme values of the radial position R are sufficient to cause a significant departure from the Wedemeyer theory, especially for small values of W. For example, a value of the aspect ratio $h/a = 5$ in a situation in which the Ekman number $E \sim 10^{-6}$ yields a minimum value of α (the value of α for which $R = 0.5$) $\alpha_{min} = 0.10$, and one would not expect times predicted by Eq. (8) to be accurate in this case. Further examples of the effect of aspect ratio on α and the consequences for spin up will be considered in the section on velocity profiles.

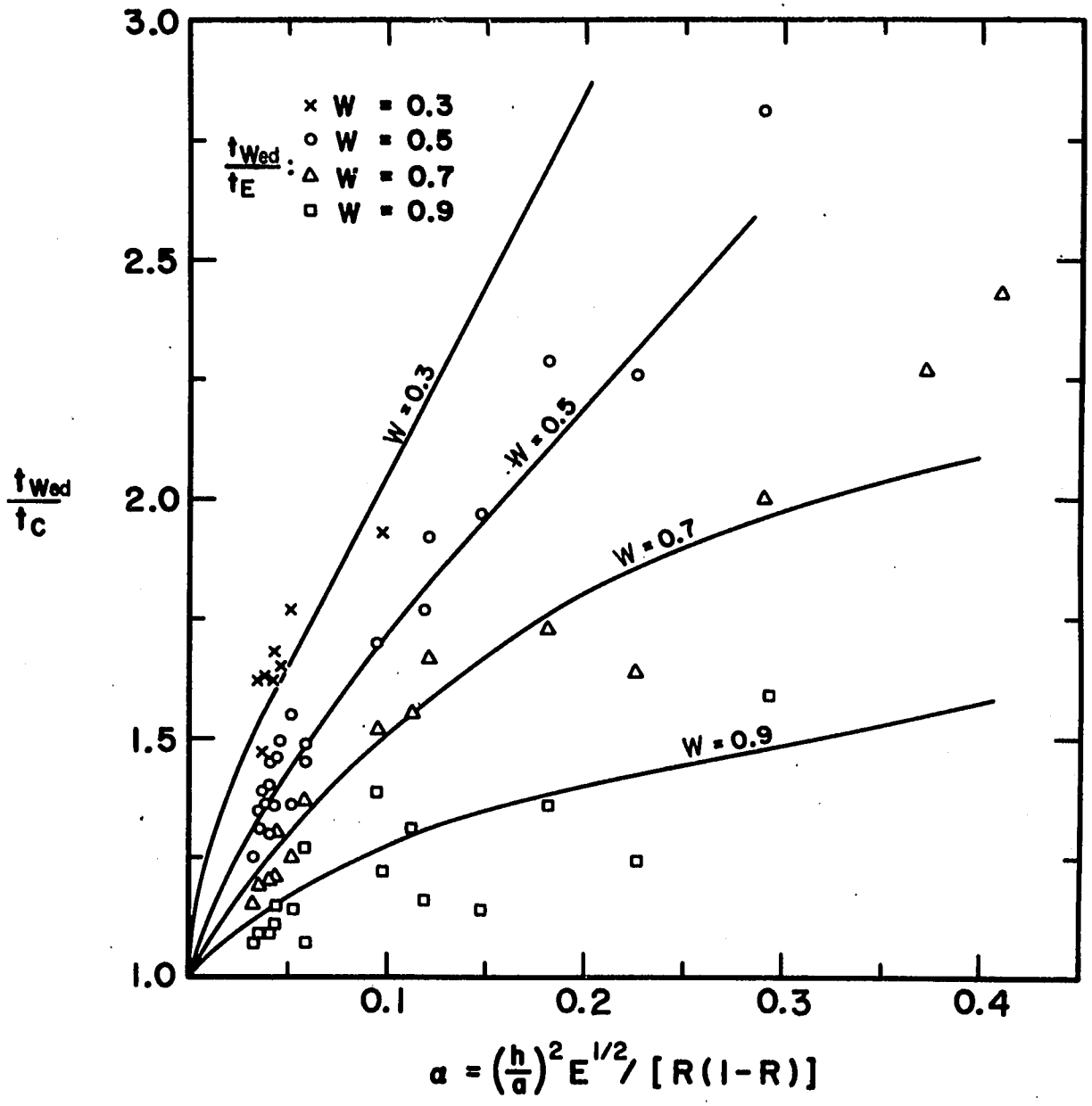
3.0
2.5
2.0
1.5
1.0
0.1
0.2
0.3
0.4
$\frac{t_{Wed}}{t_C}$
$\frac{t_{Wed}}{t_E}$:
× W = 0.3
○ W = 0.5
△ W = 0.7
□ W = 0.9
W = 0.3
W = 0.5
W = 0.7
W = 0.9
$\alpha = \left(\frac{h}{a}\right)^2 E^{1/2} / [R(1-R)]$

Fig. 8

The parameter α is relatively constant with R for intermediate values of R. The value of α increases over α_{min} by a factor of two for the radial positions R = 0.86 and R = 0.14, and the value of α increases over α_{min} by a factor of three for the radial positions R = 0.91 and R = 0.09. The value of α_{min}, therefore, is a good indication of how well Eq. (8) will predict times for different values of W in the region $0.15 \leq R \leq 0.85$.

The parameter α increases rapidly with R for radial positions $R < 0.1$ and $R > 0.9$. This is a manifestation of the importance of viscosity in the interior flow region in the very early and very late stages of the spin up. Recall from the previous section that as $\alpha >> 1$, the dimensionless time T approaches the diffusion result, $T_d = \nu t/a^2$. In the very early stages of spin up, momentum diffuses from the container wall (R = 1), and this initial diffusion is primarily responsible for the broadening of the velocity front whose position is defined by $R = e^{-T_c}$ (in the limit $\alpha \to 0$). In the very late stages of spin up, the convective circulation begins to decay as the velocity front approaches R = 0. In the absence of the convective circulation further spin up to rotation as a rigid body must occur through the mechanism of viscous diffusion.

The parameter α may also be expressed in terms of the Reynolds number $Re = a^2\Omega/\nu$:

$$\alpha = \left(\frac{h}{a}\right)(Re)^{-\frac{1}{2}}/\left[R(1 - R)\right]. \qquad (22)$$

For the physical situation defined by h = a = 4 cm., $\nu = 0.01$ cm^2/sec, and $\Omega = 1.0$/sec, a value $\alpha_{min} = 0.10$ is obtained. The aspect ratio for this case is 0(1), the Ekman number is $0(10^{-3})$ and the Reynolds number is $0(10^{3})$. Clearly the value of α_{min} caused by this small a Reynolds number indicates that the times predicted by Eq. (8) will be inaccurate.

C. Velocity Profiles

1. Comparison of Wedemeyer profiles with numerical profiles

Velocity profiles (W(R,T) obtained from both Wedemeyer's expression (Eq. (8)) and the numerical solution to Eq. (4) are presented in Figs. 9, 10, and 11. The minimum value of the dimensionless parameter α was found to be an indicator of the difference between the Wedemeyer profiles and the numerical profiles. For purposes of comparison, in these three figures time was made dimensionless by means of the convective result, i.e. $T = T_c = (\nu\Omega)^{\frac{1}{2}}h^{-1}t$.

The velocity profiles in Fig. 9 were calculated for an aspect ratio h/a = 0.5, an Ekman number $E = 2.5 \times 10^{-4}$ and a Reynolds number $Re = 1.6 \times 10^{4}$. The minimumvalue of α was $\alpha_{min} = 0.016$. Wedemeyer's expression proved to be a valid approximation for calculating velocities in this case.

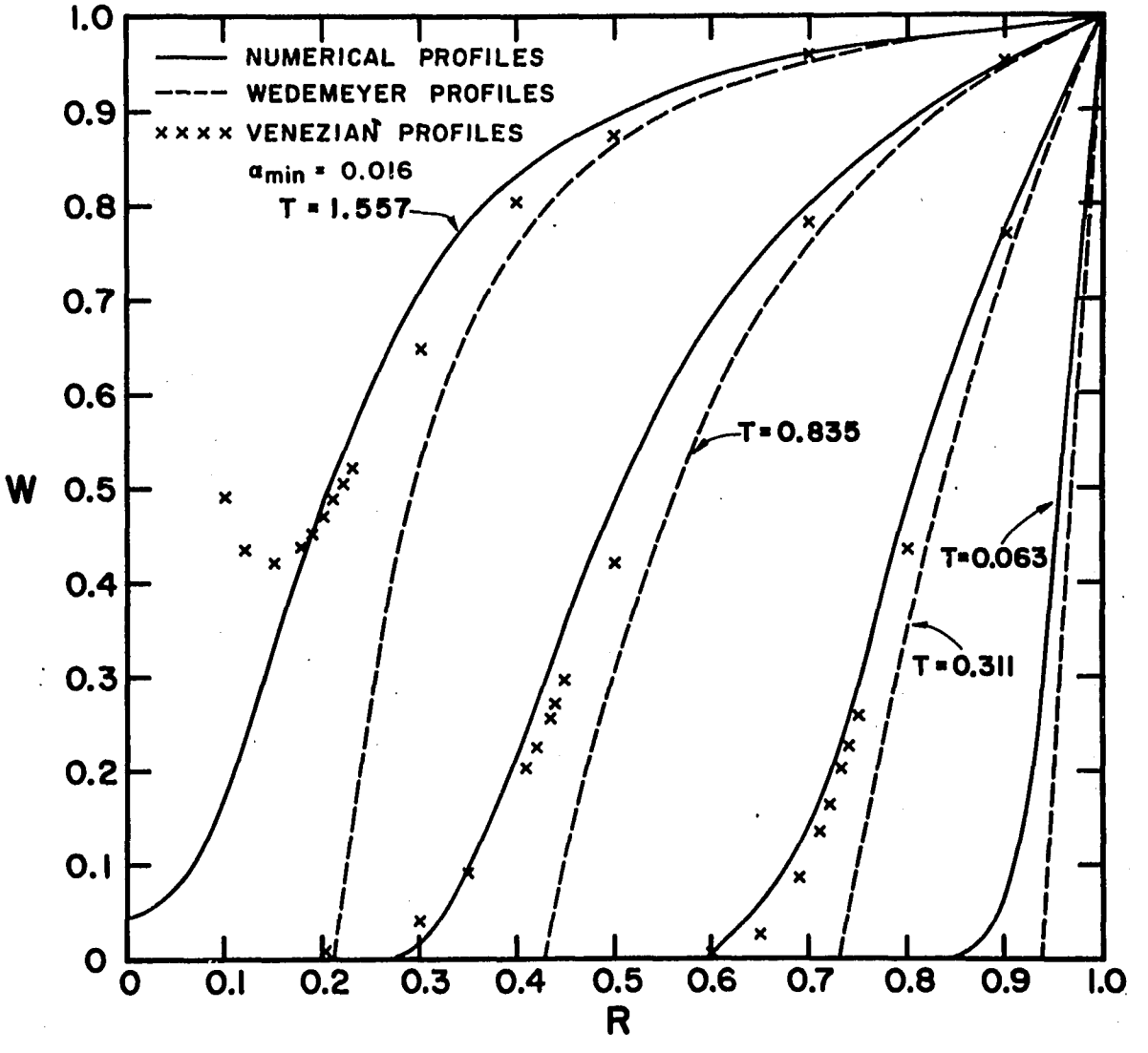
NUMERICAL PROFILES
WEDEMEYER PROFILES
×××× VENEZIAN PROFILES
a_{min} = 0.016
T = 1.557
T = 0.835
T = 0.063
T = 0.311
W
R
0
0.1
0.2
0.3
0.4
0.5
0.6
0.7
0.8
0.9
1.0

Fig. 9

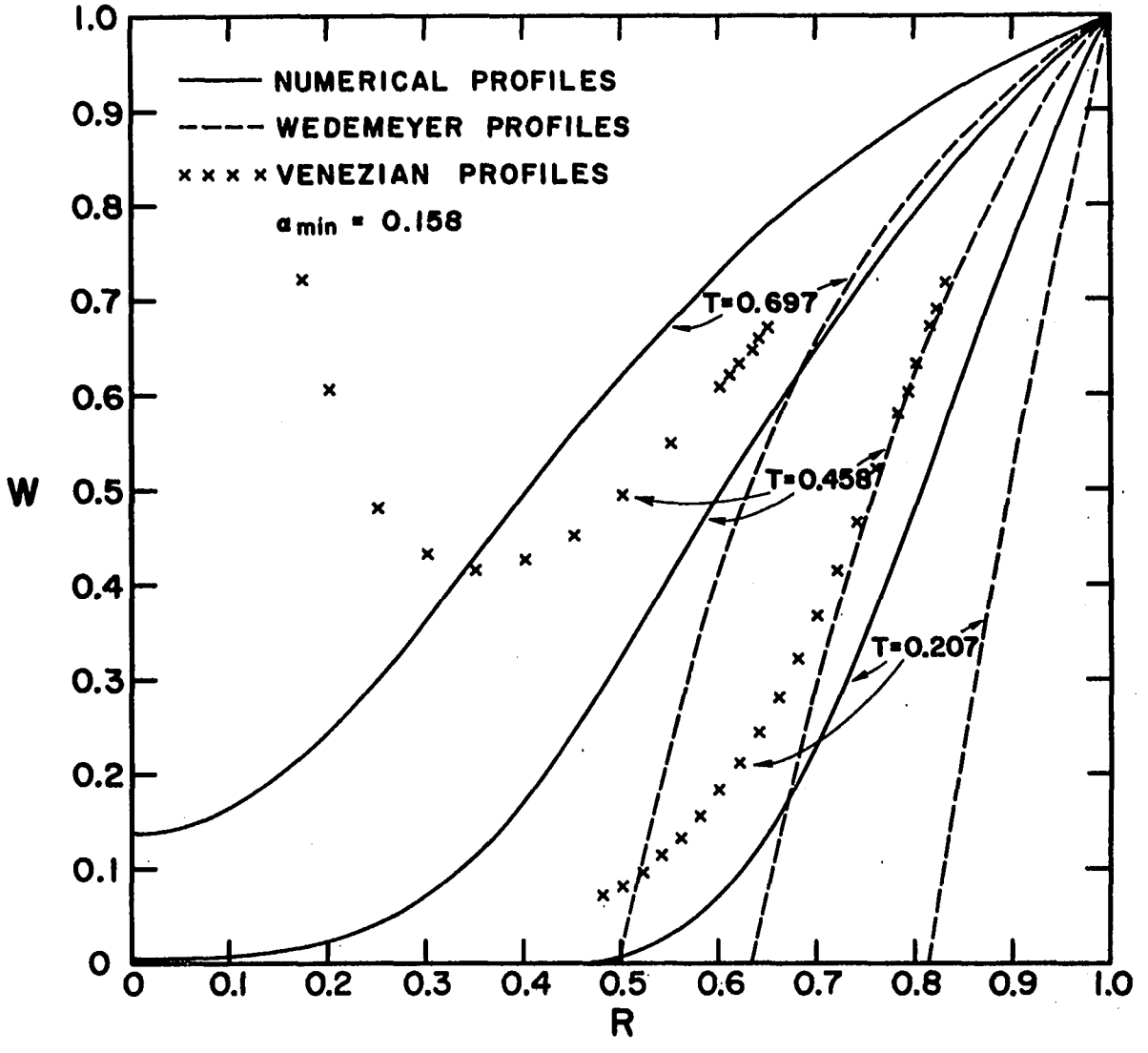
NUMERICAL PROFILES
WEDEMEYER PROFILES
VENEZIAN PROFILES
a_{min} = 0.158
T=0.697
T=0.458
T=0.207
W
R
0
0.1
0.2
0.3
0.4
0.5
0.6
0.7
0.8
0.9
1.0

Fig. 10

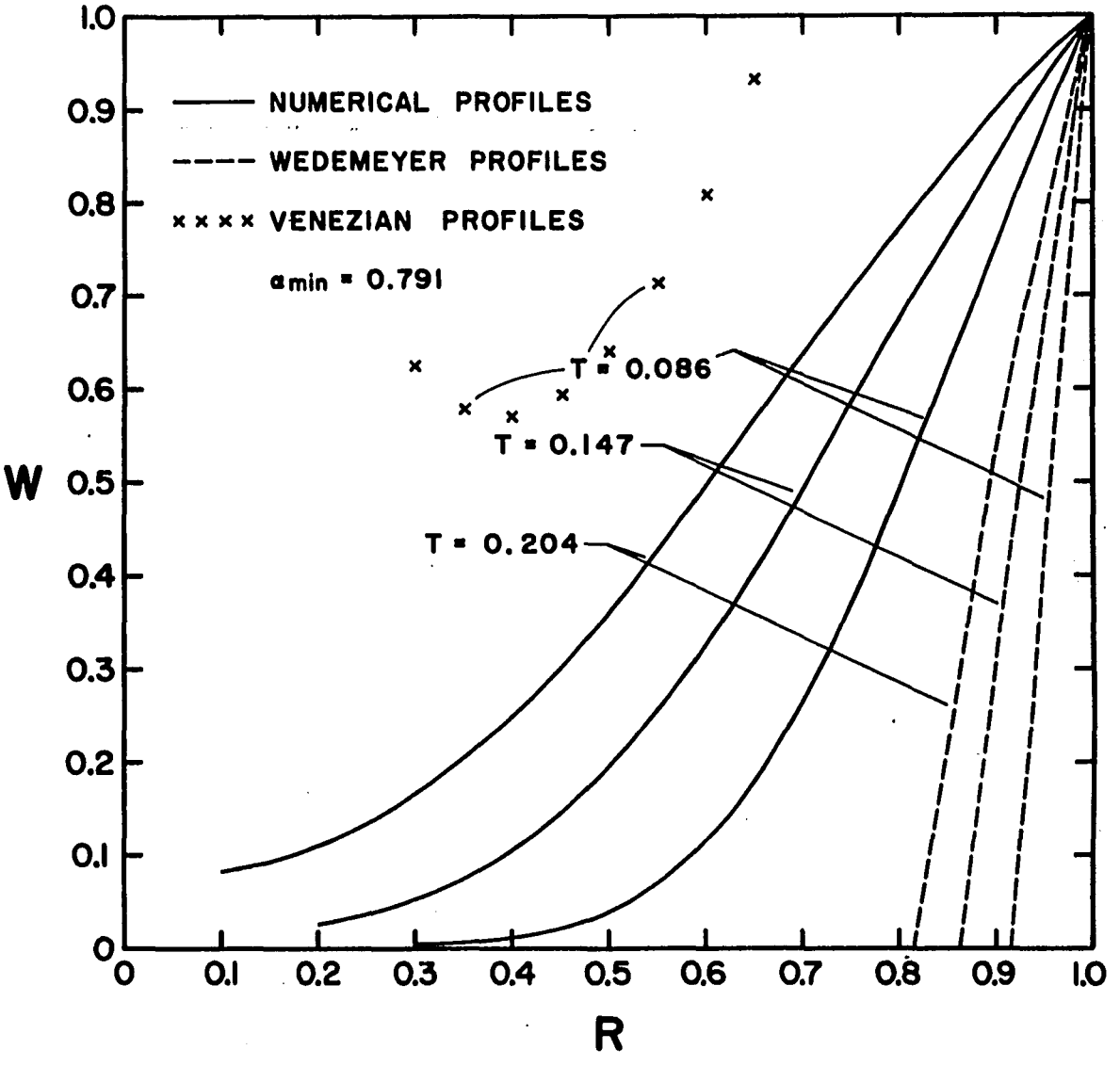
NUMERICAL PROFILES
WEDEMEYER PROFILES
VENEZIAN PROFILES
αmin = 0.791
T = 0.086
T = 0.147
T = 0.204
W
R
0
0.1
0.2
0.3
0.4
0.5
0.6
0.7
0.8
0.9
1.0

Fig. 11

The difference between the Wedemeyer profiles and the numerical profiles was found to be small for all values of both W and T. The greatest difference between the two sets of velocity profiles occurs at the velocity front $R = e^{-T}$. Wedemeyer's prediction that the effects of viscosity in the interior will act to smooth out the velocity gradient discontinuity is confirmed by the numerical profiles.

The velocity profiles in Fig. 10 were calculated for an aspect ratio $h/a = 5$, an Ekman number $E = 2.5 \times 10^{-6}$, and a Reynolds number $Re = 1.6 \times 10^{4}$. The minimum value of α was $\alpha_{min} = 0.158$, and the increase in α_{min} was caused by a ten-fold increase in aspect ratio over the example of the previous paragraph. For even this moderate value of α_{min} the velocity profiles calculated using the Wedemeyer expression differed greatly from the velocity profiles calculated numerically for all values of both W and T. One would not expect calculations based on Eq. (8) to be even approximately valid in this case.

The velocity profiles in Fig. 11 were calculated for an aspect ratio $h/a = 25$, an Ekman number $E = 1 \times 10^{-7}$, and a Reynolds number $Re = 1.6 \times 10^{4}$. The value of α_{min} was $\alpha_{min} = 0.791$, and the increase in α_{min} was caused by a five-fold increase in aspect ratio over the previous example. For this large a value of α_{min}, the Wedemeyer expression

clearly does not apply to the calculation of velocities W for any value of either W or T.

The Ekman number is defined as $E = \nu/\Omega h^2$. Since $(\nu/\Omega)^{\frac{1}{2}}$ is a measure of the thickness of the boundary layers on the ends of the cylinder, the Ekman number can be thought of as the square of the ratio of the boundary layer thickness to the height h of the cylinder. It is clear that in order for the Wedemeyer model (convection driven by transport in the boundary layers) to apply, this ratio must be small; otherwise the concept of an endwall boundary layer would be meaningless. However, it is apparent from Figs. 9-11 that smallness of the Ekman number is not a sufficient condition for the Wedemeyer model to be valid. Rather, the size of the aspect ratio h/a is much more crucial for determining the validity of the Wedemeyer solution than the size of the Ekman number. More precisely, the parameter α (which depends upon the square of the aspect ratio, but only upon the square root of the Ekman number) must be small compared to 1 in order for the Wedemeyer solution to predict accurately the velocity profiles.

2. Experimental profiles

In the experiment, velocities were measured (as a function of time) at a fixed radial position. In order to construct velocity profiles from these data, it is necessary

to decide how to connect velocities at one radial position with velocities at another radial position. One could use the dimensional time t to make this connection; however, there would still be the question of how to compare velocity profiles made under different experimental conditions, and how to compare the experimental profiles with those determined numerically (also possibly under different conditions). Earlier in this chapter, it was shown that for the numerical solutions the appropriate dimensionless time T depends upon the parameter α and upon the dimensionless angular velocity W. Therefore, it would seem reasonable to use this numerically determined time T to characterize the velocity profiles. However, such a procedure becomes quite complicated because of the dependence of T on W (see Fig. 5) and the dependence of α on the radial position R (see Eq. (18)). Since both of these dependences are weak, it was decided to use the value of α_{min} (which is independent of R) to determine T and to ignore the dependence of T on W by choosing W = 0.5. Therefore, the following procedure was used: The value of $\alpha_{min} = 4h(\nu/\Omega)^{\frac{1}{2}}/a^2$ was calculated from the experimental parameters. Then this value of α_{min} was used to determine the powers k, ℓ, m, and n from Fig. 5 (with W = 0.5). These powers were used in Eq. (15) to calculate the dimensionless time T for a given dimensional time t. Each velocity profile is then characterized by a constant

value of T. Therefore, a complete family of velocity profiles is determined by the value of the parameter α_{min}.

Measurements were performed on laboratory situations which determined small ($\approx$0.08) and intermediate ($\approx$0.22) values of α_{min}. The measured velocity profiles were compared with numerically obtained profiles for situations with slightly different values of a, h, ν, and Ω than in the experiments. However, the value of α_{min} was the same for both the numerical profiles and the experiment.

The small α_{min} in the laboratory was defined by a = 6.96 cm, h = 13.92 cm, ν = .0092 cm^2/sec and Ω = 1.83/sec. The small α_{min} in the calculations was defined by a = 7.36, h = 14.72, ν = .0089 cm^2/sec and Ω = 1.56/sec. The results of both measurements and calculations are presented in Fig. 12. The curves in Fig. 12 are labeled with dimensionless times T = T(W = 0.5, α_{min} = 0.082). The experimental points are seen to be within experimental error of the numerical curves.

The intermediate α_{min} in the laboratory was defined by a = 4.52, h = 13.70, ν = .0088 cm^2/sec and Ω = 1.34/sec. The intermediate α_{min} in the calculations was defined by a = 7.36 cm, h = 14.72 cm, ν = .0089 cm^2/sec and Ω = 1.56/sec. The results of both measurements and calculations are presented in Fig. 13. The curves are labeled with dimensionless times T = T(W = 0.5, α_{min} = 0.217). The experimental

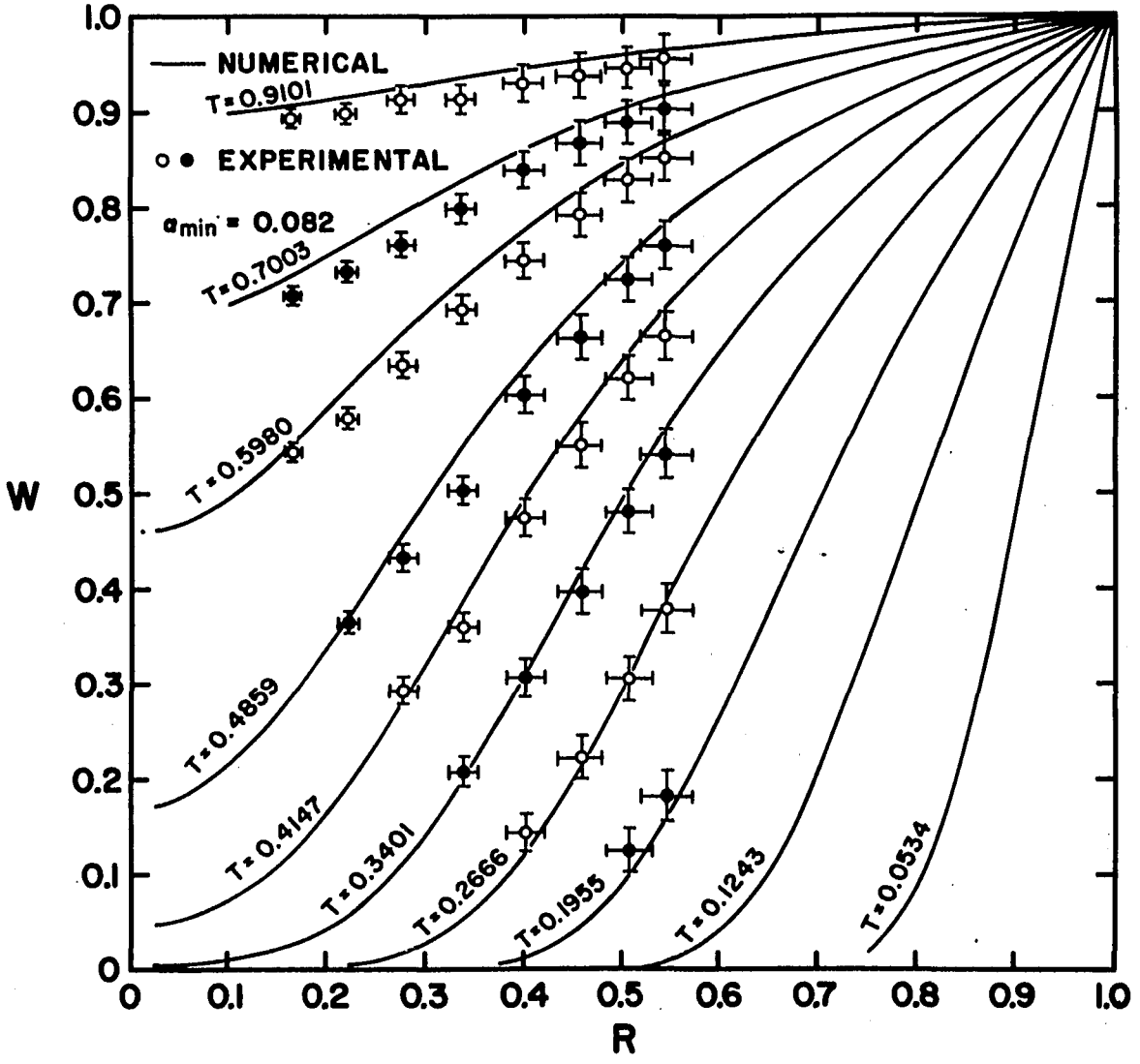
NUMERICAL
EXPERIMENTAL
a_{min} = 0.082
T=0.9101
T=0.7003
T=0.5980
T=0.4859
T=0.4147
T=0.3401
T=0.2666
T=0.1955
T=0.1243
T=0.0534
W
R
0
0.1
0.2
0.3
0.4
0.5
0.6
0.7
0.8
0.9
1.0

Fig. 12

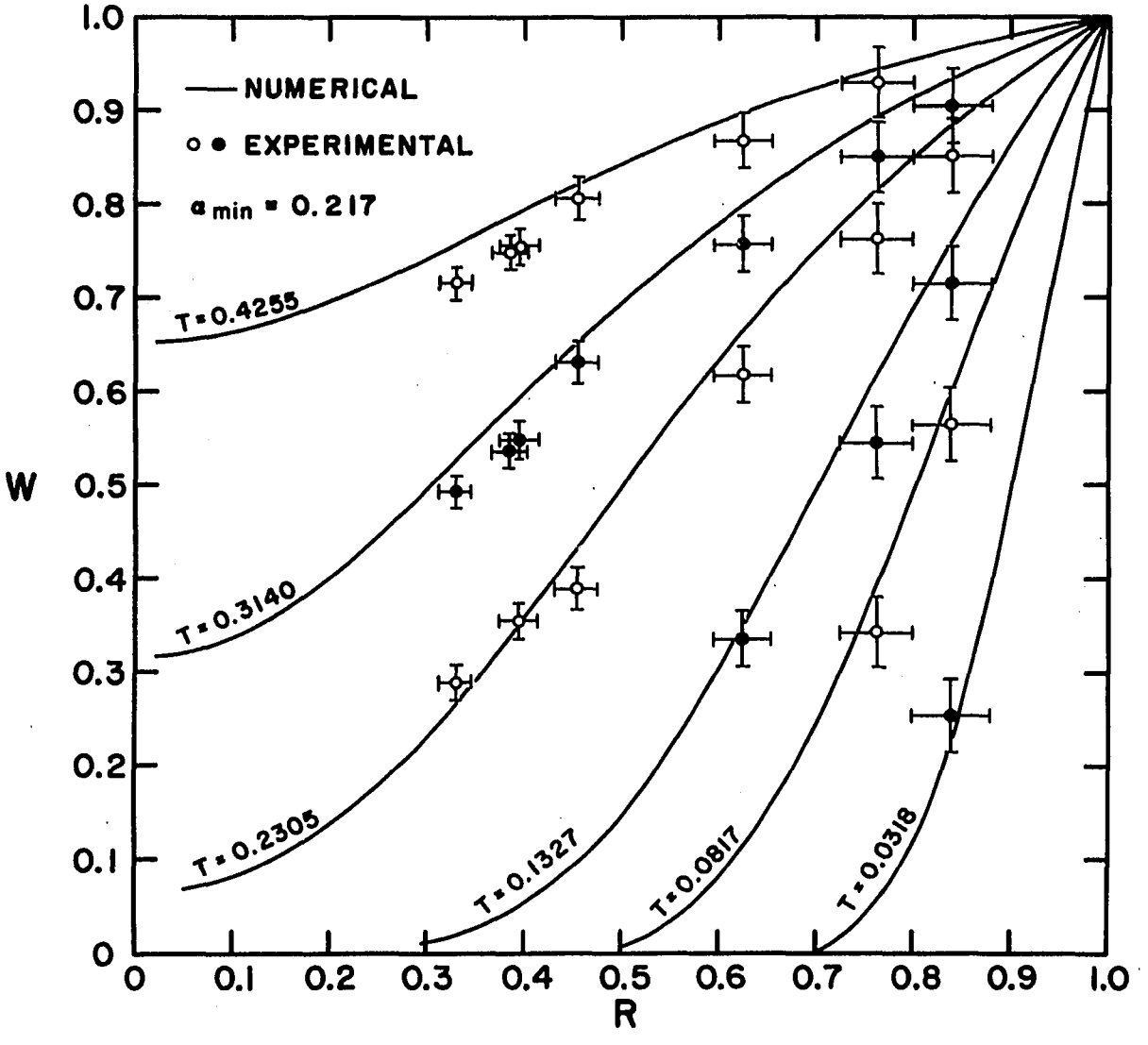
NUMERICAL
EXPERIMENTAL
α min = 0.217
T=0.4255
T=0.3140
T=0.2305
T=0.1327
T=0.0817
T=0.0318
W
R
0
0.1
0.2
0.3
0.4
0.5
0.6
0.7
0.8
0.9
1.0

Fig. 13

points are again seen to be in good agreement with the numerical result.

The results shown in Figs. 12 and 13 confirm the validity of the numerical solution of Eq. (4). It is clear that the numerical solution has a much wider range of validity than the Wedemeyer solution (compare Figs. 10 and 13). However, the difficulty of obtaining the numerical solution limits its utility. Therefore, it is useful to explore the applicability of the theory of Venezian, which is built upon the theory of Wedemeyer but includes in an approximate way the effects of viscosity in the interior. We consider Venezian's theory in section 4.

3. Axial independence of v in the interior flow region

The z-independence of the azimuthal velocity v in the interior flow region was verified by measuring the time required for the dimensionless angular velocity W to become a given value at a fixed radial position but at different axial positions. The measurements were performed at two different values of Ω at each of four different axial positions. The results are shown in Fig. 14. The height of this container was 14.72 cm. The axial independence of v in the interior, shown here experimentally, confirms the boundary-layer model used in deriving Eq. (4). Although viscosity may strongly influence v near the velocity front, it influences only the radial and not the axial variation of v.

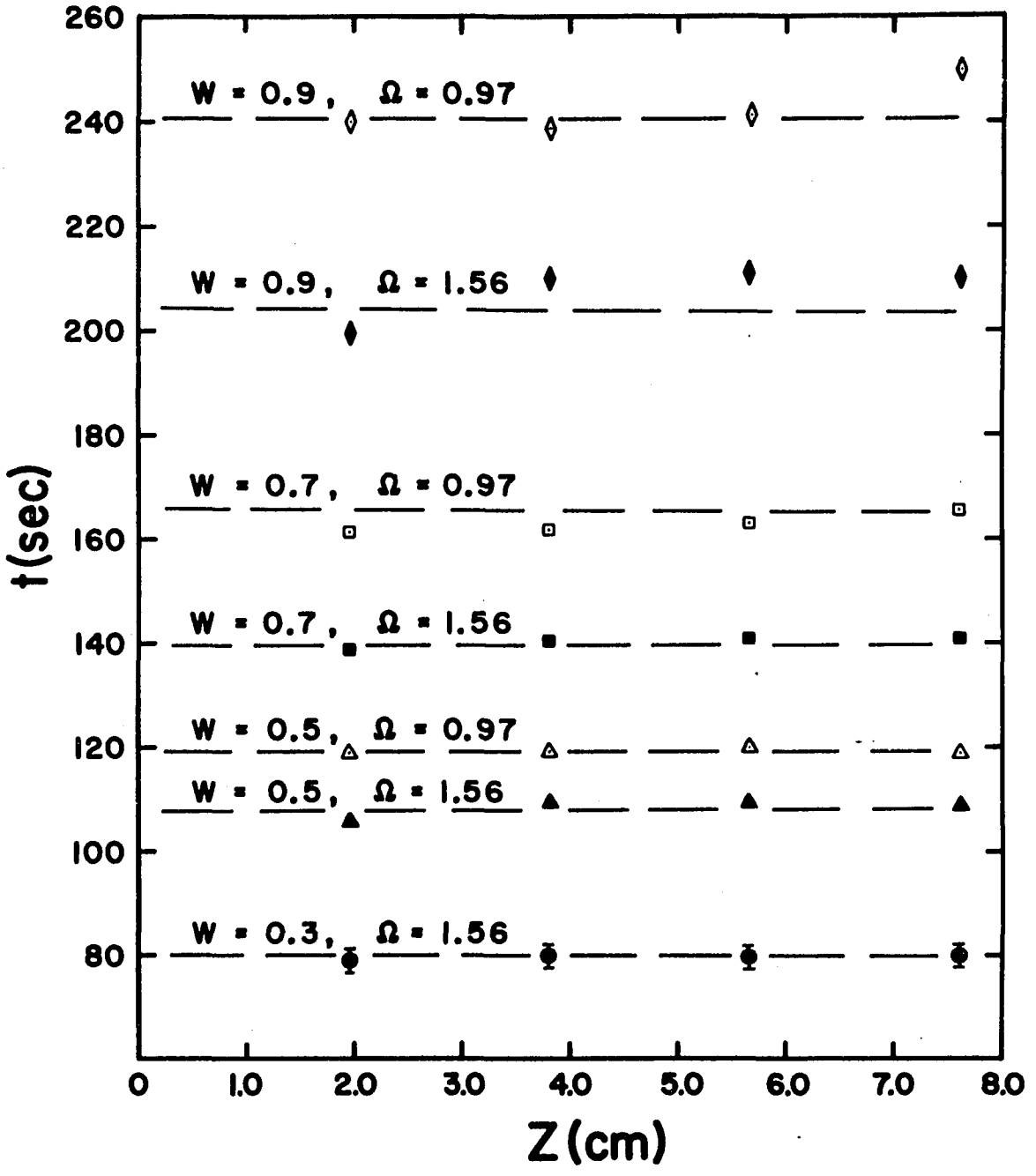
260
240
220
200
180
160
140
120
100
80
t(sec)
W = 0.9, Ω = 0.97
W = 0.9, Ω = 1.56
W = 0.7, Ω = 0.97
W = 0.7, Ω = 1.56
W = 0.5, Ω = 0.97
W = 0.5, Ω = 1.56
W = 0.3, Ω = 1.56
0
1.0
2.0
3.0
4.0
5.0
6.0
7.0
8.0
Z(cm)

Fig. 14

A photograph of the columnar nature of the interior flow in spin-up from rest is contained in Greenspan's book.[14]

4. Comparison of Venezian profiles with numerical profiles

In section 2 we showed that the experimental results were in good agreement with velocity profiles obtained from the numerical solution of Eq. (4). However, these numerical profiles are difficult to obtain, so in this section we explore the validity of a theory due to Venezian which makes calculation of profiles simpler. Venezian's theory is built upon the convection model of Wedemeyer, but includes the effect of viscosity in smoothing out the velocity front. Velocity profiles W(R,T) were calculated using Venezian's expression (Eq. (9)) for the three examples given in section 1 (Figs. 9-11). It was found that the difference between the numerical profiles and the Venezian profiles depends upon both the value of the parameter $\alpha_{min} = 4h(\nu/\Omega)^{\frac{1}{2}}/a^2$ and the value of the convective dimensionless time $T = T_c = t(\nu\Omega)^{\frac{1}{2}}/h$.

The Venezian profiles for the smallest value of α_{min} are shown in Fig. 9. The figure shows that if the time T is not too large, the Venezian profiles are very nearly identical with the numerical profiles. However, at large values of T, the Venezian profile exhibits a minimum and begins to

diverge as $R \to 0$. The Venezian profil s for intermediate and large values of α_{min} are shown in Figs. 10 and 11, respectively, for comparison with the corresponding numerical profiles. One can see from the last two figures that as α_{min} increases, the Venezian expression becomes an increasingly poorer representation of the velocity profile. Figures 9-11 show a need for a quantitative statement of the limits of applicability of Eq. (9). The remainder of this section will be directed to this goal. Three cases will be considered: a) the condition for Eq. (9) to be valid behind the Wedemeyer velocity front ($R > e^{-T}$); b) the condition for Eq. (9) to be valid ahead of the velocity front ($R < e^{-T}$); and c) the conditions for Eq. (9) to be valid both ahead and behind the front.

a) Condition for Eq. (9) to be valid behind the Wedemeyer front ($R > e^{-T}$).

Venezian has shown that as the stretched coordinate $\zeta = (R^2e^{2T} - 1)/\sqrt{\alpha_{min}}$ becomes large, the expression for the dimensionless velocity, Eq. (9), approaches the Wedemeyer solution, Eq. (8). This can be demonstrated by introducing the variable $\beta = \zeta/\sqrt{2\eta}$, where $\eta = e^{2T} - 1$. For large β, the complementary error function erfcβ can be approximated by

$$\text{erfc}\beta = e^{-\beta^2}/\beta\sqrt{\pi} \qquad \beta >> 1. \tag{23}$$

With this approximation, Eq. (9) can be written

$$W_{Ven} = V/R = \frac{4hE^{\frac{1}{4}}\ \beta\sqrt{\pi}}{r(2\pi\eta)^{\frac{1}{2}}} = \frac{R^2e^{2T} - 1}{R\eta} \qquad (24)$$

which is identical to the Wedemeyer solution. We can inquire how large β must be for the approximation to suffice by looking at the second term in the asymptotic expression for erfcβ:

$$\text{erfc}\beta = (e^{-\beta^2}/\beta\sqrt{\pi})\left[1 - (1/2\beta^2) + \ldots .\right] \qquad (25)$$

The approximation will be valid within 1% if

$$1/2\beta^2 < 0.01 \qquad (26a)$$

or

$$\alpha_{min} < 0.01(e^{2T} - 1) = 0.01\eta. \qquad (26b)$$

The quantities in Eq. (26b) for the Venezian profiles in Figs. 9-11 are presented in Table II. Only the entries on

Table II

T	α_{min}	$0.01(e^{2T}-1)$	$0.1(e^{2T}-1)$
0.311	0.016	0.0086	0.086
0.835	0.016	0.0431	0.431
1.557	0.016	0.2151	2.151
0.207	0.158	0.0051	0.051
0.458	0.158	0.0150	0.150
0.086	0.791	0.0019	0.019

the second and third lines of this table (i.e. for T = 0.835 and T = 1.557) meet the 1% criterion expressed in Eq. (26b). In both of these cases the Venezian theory (as shown in Fig. 9) does appear to give a good representation of the velocity profile for [illegible].

One may note that the conclusion drawn from Eq. (26b) for the case of T = 0.311 in Fig. 9 seems to contradict the conclusion drawn from inspection of the Venezian profile for this case. It was verified that as R → 1, the Venezian profile for T (α_{min} = 0.016) = 0.311 does not approach Eq. (24) to within 1%. However, the Venezian profile as shown in Fig. 9 in this case does constitute a very good approximation to the numerical profile. The difficulty is resolved when one realizes that for small values of T, the Venezian expression is a rapidly changing function of radial position, and the requirement that Eq. (25) holds to within 1% as R → 1 is actually too restrictive. A much more reasonable requirement for small values of T would be that Eq. (25) holds to within 10% as R → 1. In this case the inequality which must be satisfied is

$$\alpha_{min} < 0.1(e^{2T} - 1). \qquad (26c)$$

Values of $0.1(e^{2T} - 1)$ are also shown in Table II. Notice that for any given value of α_{min}, the inequality (26b) will eventually be satisfied as the time increases. Therefore, near the sidewall (R near 1), the Venezian expression will become an increasingly better representation of the velocity profile as T increases.

b) Condition for Eq. (9) to be valid ahead of the Wedemeyer front ($R < e^{-T}$).

Criteria were established for the validity of Eq. (9) for $R < e^{-T}$ in the following manner. It was observed that the Venezian profiles $W_{Ven}(R,T)$ often showed a minimum at some value of dimensionless radial position R_{min}. This is because W is proportional to $1/R^2$; Venezian demonstrated only that the momentum density $RV \to 0$ as $R \to 0$. The value of R for which W_{Ven} reaches a minimum was calculated by solving

$$\left.\frac{dW_{Ven}}{dR}\right|_{R_{min}} = 0 \qquad (27)$$

for R_{min}. It was found that near the minimum of W_{Ven}, erfcβ was only weakly dependent on R, so the approximation erfc$\beta \sim$ constant (=2) was used to simplify the calculations. A quadratic in R^2_{min} resulted from Eq. (27):

$$R^4_{min}e^{4T} - R^2_{min}e^{2T} + \alpha_{min}\eta = 0 \qquad (28)$$

where $\eta = e^{2T} - 1$. The values of R^2_{min} are found from Eq. (28) to be

$$R^2_{min} = \frac{1}{2}e^{-2T}\left[1 - (1 - 4\alpha_{min}\eta)^{\frac{1}{2}}\right] . \qquad (29)$$

This limited the values of T to those values for which

$$4\alpha_{min}\eta \leq 1. \qquad (30)$$

For values of T for which Eq. (30) is not satisfied, the values of R_{min} obtained from Eq. (29) are complex.

When $4\alpha_{min}\eta \sim 1$, the minimum value of W is about 0.26; this is much too large. Therefore, we restrict our attention to values of α_{min} and T for which $4\alpha_{min}\eta << 1$. Then

$$(1 - 4\alpha_{min}\eta)^{\frac{1}{2}} \sim 1 - 2\alpha_{min}\eta. \tag{31}$$

Equation (29) with this substitution determines R_{min}^2 to be

$$R_{min}^2 \sim \alpha_{min}\eta e^{-2T}. \tag{32}$$

This value of R_{min}^2 may be used to calculate $W_{Ven}(R_{min})$:

$$W_{Ven}(R_{min}) \sim \frac{1}{4}\sqrt{\frac{2}{\pi}}\,\frac{e^{2T}e^{-\beta^2}}{e^{2T} - 1}\,\frac{1}{\sqrt{\frac{1}{4}\alpha_{min}\eta}}. \tag{33}$$

If one requires that $W_{Ven}(R_{min}) < 0.01$, then the expression which results is

$$0.01 < \frac{1}{4}\sqrt{\frac{2}{\pi}}\,\frac{e^{2T}e^{-\beta^2}}{e^{2T} - 1}\,\frac{1}{\sqrt{\frac{1}{4}\alpha_{min}\eta}}. \tag{34}$$

This is equivalent to

$$0.01\left(\frac{1}{4}\alpha_{min}\eta\right)^{\frac{1}{2}}\,4\sqrt{\frac{\pi}{2}}\,\frac{e^{2T} - 1}{e^{2T}} > e^{-\beta^2}. \tag{35}$$

Using $4\ \frac{\pi}{2}\ 5$ and recalling the original assumption, namely that $4\alpha_{min}\eta << 1$, we have that

$$\frac{1}{4} >> \left(\frac{1}{4}\alpha_{min}\eta\right)^{\frac{1}{2}} > 20\frac{e^{2T}}{e^{2T} - 1}e^{-\beta^2}. \tag{36}$$

From the first and last terms of Eq. (36) we obtain the inequality

$$e^{\beta 2} > 80\frac{e^{2T}}{e^{2T} - 1}. \tag{37}$$

Values of $\left[\ell n\frac{80e^{2T}}{e^{2T} - 1}\right]^{\frac{1}{2}}$ for different values of T are presented in Table III.

Table III

T	$\ell n\frac{80e^{2T}}{e^{2T-1}}^{\frac{1}{2}}$
0.05	2.595
0.10	2.468
0.30	2.275
0.50	2.200
1.00	2.128
1.30	2.112
1.70	2.101
2.00	2.098

From Table IIIand Eq. (37), we see that for $W_{Ven}(R_{min})<0.01$, then $|\beta|$ is bounded below for a value of T by the entry in the second column of Table III. Consider the case for $T \geq 0.1$. Then from Table III, $|\beta| > 2.5$. From the expression for β in terms of α_{min},

$$\beta = \frac{1}{2}(R^2e^{2T} - 1)(\frac{1}{2}\alpha_{min}\eta)^{-\frac{1}{2}} \tag{38}$$

and from the fact that $\beta < 0$ for $R < e^{-T}$, we have that

$$-2\beta(\frac{1}{2}\alpha_{min}\eta)^{\frac{1}{2}} < 1 - R^2e^{2T} < 1. \tag{39}$$

Using $-\beta > 2.5$, we have that

$$(\tfrac{1}{2}\alpha_{min}{}^{n})^{\frac{1}{2}} < \frac{1}{5} \tag{40a}$$

or

$$\alpha_{min}(e^{2T} - 1) < 0.08. \tag{40b}$$

Equation (40b) provides an upper limit for values of T (at constant α_{min}) for which $W_{Ven}(R_{min}) < 0.01$. The quantities in Eq. (40b) for the Venezian profiles in Figs. 9-11 are summarized in Table IV. The criterion (40b) is met only by

Table IV

T	α_{min}	$\alpha_{min}(e^{2T}-1)$
0.311	0.016	0.0138
0.835	0.016	0.0690
1.557	0.016	0.3442
0.207	0.158	0.0806
0.458	0.158	0.2370
0.086	0.791	0.1503

the entries on the first two lines of Table IV (i.e., for T = 0.311 and T = 0.835) and it can be seen from Fig. 9 that in these two cases, the Venezian expression is a good representation of the velocity profile.

Notice that for any given value of α_{min}, the inequality (40b) will be satisfied only if the time T is sufficiently small. Therefore, ahead of the front ($R > e^{-T}$) the Venezian expression will become a progressively worse representation of the velocity front as T increases.

c) Conditions for Eq. (9) to be valid both ahead and behind the front.

Equations (26b) and (40b) may be used to obtain a range of values of T for which both $W_{Ven}(R_{min}) < 0.01$ and $W_{Ven}(R \to 1) - 1.0 < 0.01$. The expression is

$$100\ \alpha_{min} < e^{2T} - 1 < \frac{.08}{\alpha_{min}}. \tag{41}$$

This expression is much more restrictive than either (26b) or (40b) alone. Note that when

$$\alpha_{min}^{\ 2} \sim 0.0008 \tag{42a}$$

or

$$\alpha_{min} \sim 0.028 \tag{42b}$$

there exists one and only one time T ($\sim$0.67) for which both restrictions on W_{Ven} are satisfied simultaneously. As α_{min} gets smaller, the range of times satisfying (41) becomes wider. Values of the maximum and minimum times satisfying (41) for various values of α_{min} are given in Table V. Examples other than those considered in Figs. 9-11 are presented in this table. It is apparent that α_{min} must be extremely small for Venezian's expression to be uniformly valid for any appreciable range of times.

Table V

α_{min}	T_{max}	T_{min}
0.001	2.20	0.048
0.003	1.66	0.13
0.005	1.42	0.20
0.010	1.10	0.35
0.016	0.90	0.48
0.020	0.80	0.55
0.025	0.72	0.63
0.028	0.67	0.67

For values of T and α_{min} for which Eq. (41) is satisfied, the Venezian expression proves to be the simplest and most accurate way to calculate velocity profiles W(R,T) without actually performing a numerical integration of Eq. (4). In terms of α_{min}, the expressions for $W_{Ven}(R,T)$ and β are

$$W_{Ven} = \frac{2(\alpha_{min})^{\frac{1}{2}} e^{-\beta^2}}{\left[2\pi(e^{2T} - 1)\right]^{\frac{1}{2}} R^2 \operatorname{erfc}(\beta)} \tag{43}$$

where erfc is the complementary error function and β is given by

$$\beta = \frac{(R^2 e^{2T} - 1)}{\left[2\alpha_{min}(e^{2T} - 1)\right]^{\frac{1}{2}}} . \tag{44}$$

D. Summary

The parameter α, defined in Eq. (18), was found to play an important role in spin-up from rest. This parameter determines the proper form of the dimensionless time (as

shown in Fig. 6 and Eq. (15)), and determines the applicability of the Wedemeyer theory (as shown in Figs. 9, 10, and 11). Its minimum value, α_{min}, determines the validity of the Venezian theory (as shown in Eqs. (26b), (40b), and (41)). Since the factor $h(\nu/\Omega)^{\frac{1}{2}}/a^2$ in α may be interpreted as the ratio of the convective time scale to the diffusive time scale, one would expect that this ratio would qualitatively predict the relative importance of convection and diffusion. The purely empirical modification of this factor, namely multiplication by $\left[R(1 - R)\right]^{-1}$, yields the parameter α which allows quantitative predictions. However, this adds the complication that the parameter depends upon radial position in addition to container geometry, rotation rate and fluid viscosity.

The experimental results, as shown in Figs. 12 and 13, were found to be in good agreement with the numerical solution of Eq. (4) when the proper dimensionless time is used. This result confirms the boundary layer model upon which Eq. (4) is based. The approximate solution of Eq. (4) due to Wedemeyer, was found to agree with the numerical solution within 30% for $\alpha < 0.02$ except near the velocity front ($W < 0.3$). The theory of Venezian is a valuable extension of the Wedemeyer result, particularly near the velocity front. However, the Venezian theory is also limited by the

value of α_{min}. Ahead of the front, $\alpha_{min}(e^{2T} - 1)$ must be less than 0.08 for the Venezian expression to have a minimum less than 0.01 (T is the time in units of $h(\nu\Omega)^{-\frac{1}{2}}$). Behind the front, $e^{2T} - 1$ must exceed 100 α_{min} for the Venezian expression to approximate Wedemeyer's theory within 1%.

APPENDIX I

Tables of Data

A. Experimental Data

Spin-up times t(sec) were measured directly from the v(r,t) curves drawn by the strip chart recorder. A representative uncertainty for the times is ±1.5 sec. The other quantities are known to be accurate to the following: height h and radius a, ±0.005 cm; rotation rate Ω, ±0.05 sec^{-1}. The viscosity of water was determined as a function of temperature from tables. The viscosity of the sucrose solutions was measured as a function of temperature using Cannon-Fenske viscometers immersed in a constant temperature bath. The temperature of the test environment was usually constant to within ±0.2°C, giving a maximum uncertainty in viscosity of ±0.005 cm^2sec^{-1} for the sucrose solution, and 0.0002 cm^2sec^{-1} for water.

The uncertainty in the radial position r of the test point is discussed in Appendix II.

a = 7.36 cm

h(cm)	$\nu\left(\frac{cm^2}{sec}\right)$	$\Omega(sec^{-1})$	R	α	t(sec) W=0.3	W=0.5	W=0.7	W=0.9
14.72	.0088	2.34	.390	.0700	71.5	95.0	119.0	165.0
14.72	.0088	1.92	.390	.0774	78.5	104.0	132.0	183.5
14.72	.0088	1.56	.390	.0858	84.5	112.2	143.5	207.0
14.72	.0088	1.56	.277	.1018	103.0	132.7	165.2	220.5
14.72	.0088	1.92	.277	.0918	99.5	122.0	148.0	204.0
14.72	.0088	2.84	.277	.0756	92.0	109.7	131.7	175.0
14.72	.0088	2.34	.277	.0832	92.0	114.5	141.0	191.0
14.72	.0088	.97	.842	.1946	19.0	32.0	53.5	106.5
14.72	.0088	.73	.842	.2244	8.5	21.0	51.0	114.0
14.72	.0089	.73	.868	.2606	17.0	36.0	63.0	132.0
14.72	.0089	.62	.868	.2852	-	36.3	66.0	138.0
14.72	.0089	.52	.868	.3114	-	38.2	70.0	148.5
14.72	.0089	.52	.740	.1850	-	74.0	119.0	207.0
14.72	.0089	.97	.740	.1354	42.5	66.0	97.0	165.5
14.72	.0089	.73	.740	.1562	-	53.0	101.5	181.0
14.72	.0089	1.40	.625	.0924	58.0	80.0	110.0	171.5
14.72	.0089	.97	.625	.1110	60.5	90.7	120.5	199.0
14.72	.0089	.73	.625	.1280	-	99.0	141.0	228.0
14.72	.0089	.73	.475	.1204	-	124.0	173.2	259.5
14.72	.0089	1.56	.475	.0824	75.0	99.7	130.5	192.0
14.72	.0089	.97	.475	.1044	-	117.0	157.0	231.0
14.72	.0089	.97	.373	.1114	-	138.0	183.0	245.0
14.72	.0089	1.56	.373	.0878	-	122.5	153.0	212.0
14.72	.0089	3.38	.247	.0718	90.5	108.0	129.0	169.5
14.72	.0089	2.34	.247	.0864	-	120.5	147.5	194.0
14.72	.0089	1.56	.247	.1058	-	135.5	170.0	221.0
14.72	.0089	4.15	.277	.0628	80.5	96.0	114.0	151.5
14.72	.0089	3.38	.126	.1266	-	116.5	135.5	177.0
14.72	.0087	1.56	.422	.0832	80.0	109.0	171.0	208.0
14.72	.0087	.97	.422	.1054	-	119.0	164.5	240.5
14.72	.0089	.97	.744	.1362	39.5	63.8	95.5	169.0

a = 6.96 cm

13.92	.0089	.734	.838	.2331	-	37.2	74.7	180.0
13.92	.0089	1.12	.838	.1886	14.5	35.8	72.0	147.0
13.92	.0089	2.34	.382	.0751	72.1	97.9	128.1	189.3
13.92	.0089	1.56	.382	.0919	-	107.8	143.6	219.0
13.92	.0089	.85	.584	.1210	-	89.4	138.3	233.7
13.92	.0089	1.56	.584	.0893	48.0	70.2	101.3	166.0
13.92	.0092	1.56	.609	.0912	47.5	66.0	91.0	145.5
13.92	.0092	1.56	.543	.0875	56.0	76.0	105.0	161.5
13.92	.0092	1.56	.500	.0883	64.5	86.0	115.5	183.0
13.92	.0092	1.56	.457	.0889	70.5	91.0	123.0	187.0
13.92	.0092	1.56	.399	.0920	81.0	104.0	133.0	198.0
13.92	.0092	1.56	.337	.0988	91.5	114.0	145.0	204.0

a = 6.96 cm

h(cm)	$\nu\left(\frac{cm^2}{sec}\right)$	$\Omega(sec^{-1})$	R	α	t(sec) W=0.3	W=0.5	W=0.7	W=0.9
13.92	.0092	1.56	.276	.1104	99.0	124.0	150.0	212.0
13.92	.0092	1.56	.220	.1286	-	130.5	158.0	213.0
13.92	.0092	1.56	.164	.1620	-	133.0	165.0	220.0
13.92	.0092	1.83	.164	.1486	-	125.0	153.0	191.0
13.92	.0092	1.83	.220	.1187	-	123.0	150.0	202.5
13.92	.0092	1.83	.276	.1020	94.0	115.5	143.0	196.0
13.92	.0092	1.83	.337	.0912	86.0	108.5	135.5	195.0
13.92	.0092	1.83	.399	.0850	75.0	95.0	125.0	183.0
13.92	.0092	1.83	.457	.0821	66.5	86.5	113.5	176.5
13.92	.0092	1.83	.504	.0815	59.5	78.0	104.5	163.0
13.92	.0092	1.83	.543	.0821	53.0	71.5	96.5	155.0
13.92	.0092	1.83	.500	.0815	61.0	82.5	114.0	218.0

a = 4.52 cm

18.06	.0089	1.56	.921	.9214	4.0	13.7	27.2	65.5
18.06	.0089	1.12	.921	1.0876	-	13.3	30.3	73.5
18.06	.0089	1.12	.725	.3962	-	37.0	68.0	127.5
18.06	.0089	1.56	.725	.3276	-	38.6	62.0	126.0
18.06	.0089	1.56	.641	.2926	-	60.0	88.0	145.5
18.06	.0089	2.34	.641	.2372	34.8	54.0	76.2	122.0
18.06	.0089	2.34	.482	.2182	-	74.0	100.2	152.5
18.06	.0089	3.38	.482	.1816	47.0	65.0	87.0	126.0
18.06	.0089	3.38	.309	.2124	-	79.2	103.5	145.0
18.06	.0089	2.34	.309	.2554	-	85.5	116.0	163.5
14.72	.0089	1.56	.457	.2196	-	73.5	106.5	159.0
14.72	.0089	1.56	.366	.2346	-	-	112.0	168.0
14.72	.0089	1.56	.590	.2248	35.0	55.0	81.5	136.5
14.72	.0089	2.34	.475	.1786	49.5	68.5	94.0	139.0
6.42	.0089	1.56	.574	.0994	-	30.0	44.7	75.0
8.04	.0089	1.56	.574	.1244	-	36.7	55.0	91.3
9.34	.0089	1.56	.574	.1510	-	39.7	60.3	102.0
10.64	.0089	1.56	.574	.1648	-	43.7	66.5	110.5
11.64	.0089	1.56	.574	.1806	-	45.0	71.0	117.5
13.72	.0089	1.56	.574	.2124	-	45.5	76.6	130.5
14.89	.0089	1.56	.574	.2294	-	46.0	77.5	134.0
16.11	.0089	1.56	.574	.2484	-	50.5	83.2	141.0
16.88	.0089	1.56	.574	.2612	-	54.3	86.7	146.0
18.06	.0089	1.56	.574	.2796	-	57.2	90.7	156.5
5.33	.0093	1.92	.578	.0748	16.0	23.4	33.4	56.5
8.08	.0093	1.92	.578	.1136	21.4	32.4	46.4	80.8
10.10	.0093	1.92	.578	.1420	-	37.4	53.8	94.6
13.98	.0093	1.92	.578	.1964	-	43.8	67.8	121.1
18.06	.0093	1.92	.578	.2532	-	53.2	80.5	143.5
4.83	.0093	1.24	.811	.1340	-	13.0	21.8	45.5

a = 4.52 cm

h(cm)	$\nu\left(\frac{cm^2}{sec}\right)$	$\Omega(sec^{-1})$	R	α	t(sec) W=0.3	W=0.5	W=0.7	W=0.9
7.27	.0093	1.24	.811	.2010	-	14.8	27.5	55.5
9.45	.0093	1.24	.811	.2618	-	17.8	33.1	76.0
11.61	.0093	1.24	.811	.3220	-	20.2	38.0	87.5
14.59	.0093	1.24	.811	.4040	-	21.7	42.4	101.0
18.06	.0093	1.24	.811	.5000	-	24.8	49.5	119.3
4.84	.0093	2.12	.413	.0628	-	32.9	42.8	62.5
6.03	.0093	2.12	.413	.0810	-	39.2	50.8	77.2
7.73	.0093	2.12	.413	.1038	-	48.0	62.5	94.3
10.26	.0093	2.12	.413	.1166	-	58.2	76.1	112.6
14.22	.0093	2.12	.413	.1900	-	70.3	94.7	141.7
18.06	.0093	2.12	.413	.2420	-	79.5	109.7	167.2
4.83	.017	2.12	.395	.0886	-	22.1	29.8	48.5
4.83	.017	2.84	.395	.0764	-	19.8	26.5	44.5
8.53	.017	2.84	.395	.1300	-	29.5	39.5	63.3
8.53	.017	2.12	.395	.1566	-	32.9	45.8	70.5
12.95	.017	2.12	.395	.2370	-	41.8	59.0	92.0
12.95	.017	2.84	.395	.2052	-	38.9	52.3	80.5
16.16	.017	2.84	.395	.2566	-	45.4	59.0	92.8
16.16	.017	2.12	.395	.2968	-	47.3	66.4	101.8
5.57	.017	2.12	.616	.1034	9.7	15.5	23.0	40.8
7.69	.017	2.12	.616	.1428	11.5	18.3	27.3	52.0
10.60	.017	2.12	.616	.1968	13.0	22.3	34.5	64.0
16.27	.017	2.12	.616	.3020	18.6	29.2	45.5	89.7
7.22	.017	1.56	.867	.3200	-	6.0	13.9	35.7
10.48	.017	1.56	.867	.4640	-	8.9	18.7	48.0
13.68	.017	1.56	.867	.6040	-	9.5	20.0	59.8
18.37	.017	1.56	.867	.8120	-	10.2	22.8	74.5
6.73	.0091	1.56	.718	.1248	-	29.0	43.2	92.7
6.73	.0091	1.12	.718	.1468	-	33.5	58.5	146.0
13.40	.0091	1.12	.718	.2910	-	51.7	90.0	222.0
13.40	.0091	1.56	.718	.2476	-	44.5	71.2	141.5
18.37	.0091	1.56	.718	.3400	-	52.7	87.0	170.5
18.37	.0091	1.12	.718	.4020	-	56.2	104.0	241.5
18.37	.0091	1.24	.718	.3820	-	53.2	94.5	214.0
18.37	.0091	1.92	.718	.3060	25.7	47.0	75.0	137.2
13.70	.0089	1.34	.385	.2313	-	84.0	112.5	165.0
13.70	.0089	1.34	.455	.2209	-	73.8	98.0	154.0
13.70	.0089	1.34	.535	.2202	47.0	67.0	95.5	151.5
13.70	.0089	1.34	.628	.2344	34.0	51.2	77.0	135.0
13.70	.0089	1.34	.765	.3047	20.0	33.5	54.3	103.5
13.70	.0089	1.34	.841	.4096	11.0	19.5	35.5	87.0
13.70	.0089	1.34	.395	.2292	59.0	81.0	108.5	162.5
13.70	.0089	1.34	.333	.2466	62.5	88.5	117.0	174.0

a = 4.43 cm

h(cm)	$\nu\left(\frac{cm^2}{sec}\right)$	$\Omega(sec^{-1})$	R	α	t(sec) W=0.3	W=0.5	W=0.7	W=0.9
11.69	.0094	1.24	.772	.2946	-	23.5	45.5	100.0
11.69	.0094	1.92	.772	.2366	-	21.0	37.7	78.8
17.90	.0094	1.92	.772	.3624	-	24.4	46.8	103.3
17.90	.0094	1.24	.772	.4510	-	31.4	61.0	140.0
28.66	.0094	1.24	.772	.7200	-	34.8	70.5	166.0
28.66	.0094	1.92	.772	.5800	-	32.5	64.3	140.5
39.90	.0094	1.92	.772	.8200	-	35.4	73.8	161.7
39.90	.0094	1.74	.772	.8500	-	31.1	65.3	150.0
39.90	.0094	1.24	.772	1.0080	-	36.2	78.0	170.0

B. Numerical Data and Computer Program

The spin-up times presented in this section were calculated using the computer program at the end of the section.

$a = 4.0$ cm; $\nu = 0.01$ cm^{2}sec^{-1}; $\Omega = 10.0$ sec^{-1}

h/2(cm)	R	α	t(W=0.5)(sec)
1.0	.955	.0920	0.3994
1.0	.905	.0460	0.9261
1.0	.855	.0319	1.4488
1.0	.805	.0252	1.9675
1.0	.755	.0214	2.4865
1.0	.705	.0190	3.0108
1.0	.655	.0175	3.5458
2.0	.955	.1840	0.6996
2.0	.905	.0920	1.7031
2.0	.855	.0638	2.7144
2.0	.805	.0504	3.7212
4.0	.955	.3679	1.1270
4.0	.905	.1839	2.9435
4.0	.805	.1007	6.7220
4.0	.705	.0760	10.5106
4.0	.605	.0662	14.3476
4.0	.505	.0633	18.2909
4.0	.405	.0656	22.3722
4.0	.205	.0970	30.4340
4.0	.105	.1682	33.3100
7.0	.955	.6439	1.5340
10.0	.905	.4598	5.2807
10.0	.805	.2518	13.1126
10.0	.705	.1901	21.0851
10.0	.505	.1581	36.6835
10.0	.405	.1640	44.0643
40.0	.905	1.8391	8.9174
40.0	.805	1.0073	25.4700
50.0	.905	2.2988	9.3574
50.0	.805	1.2592	27.2151
50.0	.705	.9504	46.6023
50.0	.605	.8270	64.4252
100.0	.905	4.5977	10.3902
100.0	.805	2.5181	31.5862

$h/2 = 1.0$ cm; $\nu = 0.01$ cm^{2}sec^{-1}; $\Omega = 10.0$ sec^{-1}

a(cm)	R	α	t(W=0.5)(sec)
2.0	.955	.3680	0.2816
2.0	.905	.1838	0.7352
2.0	.855	.1274	1.2054
2.0	.805	.1006	1.6771
2.0	.755	.0856	2.1484
2.2	.955	.3040	0.3019
2.2	.905	.1520	0.7714
2.2	.855	.1054	1.2536
2.2	.805	.0832	1.7359
2.2	.755	.0708	2.2177
4.5	.955	.0726	0.4119
4.5	.905	.0362	0.9436
4.5	.855	.0252	1.4698
4.5	.805	.0198	1.9916
4.5	.755	.0588	2.5140
5.0	.955	.0588	0.4213
5.0	.905	.0294	0.9566
5.0	.855	.0204	1.4851
5.0	.805	.0162	2.0091
5.0	.755	.0138	2.5338

$h/2 = 2.0$ cm; $\nu = 0.01$ cm^{2}sec^{-1}; $\Omega = 10.0$ sec^{-1}

2.0	.955	2.3270	0.5940
2.0	.905	1.1630	1.9530
2.0	.855	.8066	3.5820
2.0	.805	.6370	5.3130
2.0	.755	.5406	7.0730
2.2	.955	1.9230	0.6880
2.2	.905	.9618	2.2150
2.2	.855	.6664	4.0150
2.2	.805	.5264	5.9120
2.2	.755	.4466	7.8360

$h/2 = 50.0$ cm; $\nu = 0.01$ cm^{2}sec^{-1}; $\Omega = 10.0$ sec^{-1}

1.0	.905	36.7814	0.7137
1.0	.805	20.1450	2.2534
1.0	.705	15.2052	3.9897
1.0	.405	13.1228	8.2627
1.0	.305	14.9180	9.1563
1.0	.205	19.4038	9.7795
1.0	.105	33.6494	10.1450
2.0	.905	9.1953	2.7334
2.0	.805	5.0362	8.4623

$h/2 = 50.0$ cm; $\nu = 0.01$ $cm^2 sec^{-1}$; $\Omega = 10.0$ sec^{-1}

a(cm)	R	α	t(W=0.5)(sec)
2.0	.705	3.8012	14.8574
2.0	.405	3.2807	30.7574
2.0	.305	3.7292	34.1319
2.0	.205	4.8508	36.4935
2.0	.105	8.4134	37.8843
5.0	.965	3.7451	2.5184
10.0	.985	2.1403	1.7120
10.0	.965	.9363	6.9794
10.0	.905	.3678	29.5296
20.0	.985	.5351	3.8459
40.0	.905	.0230	49.3047

$h/2 = 2.0$ cm; $a = 4.0$ cm; $\Omega = 1.0$ sec^{-1}

$\nu(cm^2 sec^{-1})$	R	α	t(W=0.5)(sec)
.11	.955	1.9294	0.2070
.11	.905	.9644	0.6660
.11	.855	.6688	1.2080
.11	.805	.5282	1.7790
.11	.755	.4483	2.3580
.12	.955	2.0152	0.1920
.12	.905	1.0073	0.6200
.12	.855	.6985	1.1280
.12	.805	.5517	1.6640
.12	.755	.4682	2.2070

$h/2 = 2.0$ cm; $a = 4.0$ cm; $\Omega = 10$ sec^{-1}

.04	.955	.3679	0.2816
.04	.905	.1839	0.7352
.04	.855	.1275	1.2054
.04	.805	.1007	1.6771
.10	.955	.5817	0.1457
.10	.905	.2908	0.4025
.10	.855	.2017	0.6764
.10	.805	.1593	0.9536
.10	.505	.1000	2.6182
.12	.955	.6373	0.1271
.12	.905	.3185	0.3552
.12	.855	.2209	0.6001
.12	.805	.1745	0.8485
.40	.505	.2000	1.0561

$h/2 = 50.0$ cm; $a = 4.0$ cm; $\Omega = 10.0$ sec^{-1}

$\nu(cm^2sec^{-1})$	R	α	t(W=0.5)(sec)
.04	.905	4.5977	2.5825
.04	.805	2.5181	7.7885
.04	.705	1.9006	13.5129
.10	.905	7.2696	1.0753
.10	.805	3.9815	3.2986
.10	.705	3.0052	5.7637
.40	.905	14.5391	0.2788
.40	.805	7.9631	0.8697
.40	.705	6.0103	1.5309
.10	.505	2.5003	10.1904
.10	.405	2.5936	11.8940
.10	.305	2.9485	13.2007
.10	.205	3.8349	14.1153
.10	.105	6.6507	14.6527
.40	.505	5.0005	2.7127
.40	.405	5.1873	3.1628
.40	.305	5.8969	3.5064
.40	.205	7.6699	3.7463
.40	.105	13.3014	3.8870

$h/2 = 14.45$ cm; $a = 7.36$ cm; $\nu = 0.17$ cm^2sec^{-1}

$\Omega(sec^{-1})$	R	α	t(W=0.5)(sec)
2.77	.955	3.0755	0.4999
2.77	.905	1.5373	1.6895
2.77	.855	1.0661	3.1503
2.77	.805	.8420	4.7211
5.54	.905	1.0870	1.5242
5.54	.805	.5954	4.1267
13.85	.905	.6875	1.2763
13.85	.805	.3765	3.2963

```
C       SPIN UP TIMES
C       A=RADIUS,H=HALF DEPTH,VIS=VISCOSITY,OMEGA=
C       ANGULAR SPEED
C       SSTAR IS THE RADIUS AT WHICH CONDITIONS ARE MET
C       OMLVL IS THE VELOCITY AT WHICH CONDITIONS ARE MET
C       FINCR IS THE INCREMENT IN RADIUS TO THE NEXT
C       SET OF DESIRED CONDITIONS
C       STOPRA IS THE RADIUS AT WHICH CALCULATIONS CEASE
C       READ O(1,J) J=1,JMAX IS THE INITIAL PROFILE
        DIMENSION O(2,1000)
        CALL ERRSET(208,256,-1,1)
        WRITE(6,67)
   67 FORMAT(3X,'RADIUS',4X,'HEIGHT',4X,'VISCOSITY',
       /2X,'ANG SPEED')
        READ(5,2)A,H,VIS,OMEGA
         WRITE(6,2)A,H,VIS,OMEGA
    2 FORMAT(1X,4(2X,F8.4))
        WRITE(6,68)
   68 FORMAT(1X,'SSTAR',5X,'OMLVL',5X,'FINCR',5X,'STOPRA')
        READ(5,4)SSTAR
        READ(5,4)OMLVL
        READ(5,4)FINCR
        READ(5,4)STOPRA
    4 FORMAT(F10.0)
        WRITE(6,69)SSTAR,OMLVL,FINCR,STOPRA
   69 FORMAT(1X,F5.3,3(5X,F5.3))
        JMAX=199
        AJMAX=JMAX
        NMAX=JMAX+1
        O(1,1)=0.
        DO 10 J=2,JMAX
   10 READ(5,92) O(1,J)
   92 FORMAT(20X,E14.7)
        O(1,NMAX)=1.
        X0=.44223C
        REN=A*A*CMEGA/VIS
        F=SQRT(VIS*OMEGA)/H
        DELX=1./NMAX
        DELT=1./100C.
        B3=VIS/(A*DELX)
        C=DELT/OMEGA
        K=1
   98   O(2,NMAX)=1.
        DO 18 J=2,JMAX
        BJ=J-1
        RR=A*BJ*DELX
        RSTAR=BJ*DELX
        Y1=0.536161*O(1,J)
        Y2=8.80327*O(1,J)
        Y3=2.528307*O(1,J)
        Y4=1.609258*O(1,J)
```

```
      Y5=0.993635*O(1,J)
      Y6=0.550504*O(1,J)
      Z1=1.-0.231796*O(1,J)
   55 U=X0+Y1*(1.-Y2*(1.-Y3*(1.-Y4*(1.-Y5*(1.-Y6*Z1)))))
      RU=U*F*RR
      B1=C/RR
      B2=BJ/A
      DELO=O(1,J+1)-O(1,J)
      DELO2=DELO-O(1,J)+O(1,J-1)
      O(2,J)=O(1,J)+B1*(RU*(BJ*DELO+2.*O(1,J))+B3*
     /(BJ*DELO2+3.*DELO))
      IF(O(2,J)-1.001)100,100,150
  150 WRITE(6,70)J,K,O(2,J)
   70 FORMAT(1X,2I5,E16.7)
      GO TO 12
  100 IF(O(2,J).GE.OMLVL.AND.ABS(RSTAR-SSTAR).LE.0.003)
     /GO TO 15
   18 CONTINUE
      O(2,1)=O(2,2)
      DO 14 L=1,NMAX
   14 O(1,L)=O(2,L)
      K=K+1
      GO TO 98
   15 AK=K
      TIME=AK*DELT/OMEGA
      WRITE(6,71)
   71 FORMAT(1X,'REYNOLDS NO.',13X,'TIME')
      WRITE(6,16)REN,TIME
   16 FORMAT(1X,2(1X,E16.7))
      WRITE(6,72)
   72 FORMAT(9X,'DRAD',13X,'O(2,M)',11X,'C(1,M)',12X,'U')
      DO 63 M=2,NMAX
      AM=M
      DRAD=AM/(AJMAX+1.)
      WRITE(7,65)DRAD,O(2,M)
   65 FORMAT(2(3X,E14.7))
   63 WRITE(6,64)DRAD,O(2,M),O(1,M),U
   64 FORMAT(1X,4(3X,E14.6))
      SSTAR=SSTAR-FINCR
      IF(SSTAR-STOPRA)12,12,18
   12 WRITE(6,66)
   66 FORMAT('END OF JOB')
      STOP
      END
```

APPENDIX II

Error Analysis

The radial position of the test point was determined by measurements of the angles ϕ_1 and ϕ_2 with the expression:

$$r = \frac{a}{2} \frac{\sin\left(\frac{\phi_1 - \phi_2}{2}\right)}{\sin\left(\frac{\phi_1 + \phi_2}{4}\right)\cos\left(\frac{\phi_1 - \phi_2}{4}\right)} \quad . \tag{1}$$

Since $\phi_1 + \phi_2$ was usually about eight degrees of arc, small angle approximations may be used; then

$$r \simeq a\left(\frac{\phi_1 - \phi_2}{\phi_1 + \phi_2}\right) \quad . \tag{2}$$

The uncertainty $\frac{\Delta a}{a}$ in the radius of the cylinder is negligible compared with the uncertainty in angles. Therefore

$$\frac{\Delta r}{r} = \left\{\left[\frac{\Delta\left(\frac{\phi_1 - \phi_2}{\phi_1 + \phi_2}\right)}{\left(\frac{\phi_1 - \phi_2}{\phi_1 + \phi_2}\right)}\right]^2\right\}^{\frac{1}{2}} \quad . \tag{3}$$

Using $$\Delta\left(\frac{\phi_1 - \phi_2}{\phi_1 + \phi_2}\right) = \frac{2(\phi_2\Delta\phi_1 - \phi_1\Delta\phi_2)}{(\phi_1 + \phi_2)^2} \tag{4}$$

then $$\frac{\Delta\left(\frac{\phi_1 - \phi_2}{\phi_1 + \phi_2}\right)}{\left(\frac{\phi_1 - \phi_2}{\phi_1 + \phi_2}\right)} = \frac{-2\Delta\phi_1}{\phi_1 + \phi_2} \quad . \tag{5}$$

The least count of the vernier-disc was six minutes of arc, and two measurements were required to determine each of ϕ_1 and ϕ_2; therefore $\Delta\phi_1 = \Delta\phi_2 = 12'$. The sum $\phi_1 + \phi_2$ was usually about eight degrees of arc. Using the substitutions

$$\frac{\Delta r}{r} \sim \frac{24'}{8^o} = 5\% \ . \tag{6}$$

Using the method outlined in the description of the experiment to calculate f_D, one may show that this is the principal contribution to the error in velocity; therefore $\Delta v/v \sim 5\%$.

If the bisector of the laser beams does not exactly pass through the axis of rotation, then the measured velocity v' is given by

$$v' = u \sin\gamma + v \cos\gamma \tag{7}$$

where u and v are the radial and tangential velocities, respectively, and γ is a small angle. Let d be the small distance the test point is displaced from a diameter parallel to the beam bisector. Then

$$\gamma \sim \frac{d}{r} \tag{8}$$

and

$$v' - v = \Delta v = u\frac{d}{r} \tag{9}$$

and

$$\frac{\Delta v}{v} = \left(\frac{u}{v}\right)\left(\frac{d}{r}\right) \ . \tag{10}(10)$$

Since $d << r$ and $\frac{u}{v} \sim O(E^{\frac{1}{2}})$, this contribution to the errorrror in velocity is quite small.

The error in velocity incurred by a slight deviation of the plane of the laser beams from perpendicular to the axis of rotation is found to be quite small in a similar manner.

APPENDIX III

Electronics

The active band pass filter in the following schematic is a modification of a design by Caplan and Stern.[13] The clipper and photomultiplier-preamplifier schematics are standard arrangements. All resistances are in ohms and all capacitances are in microfarads.

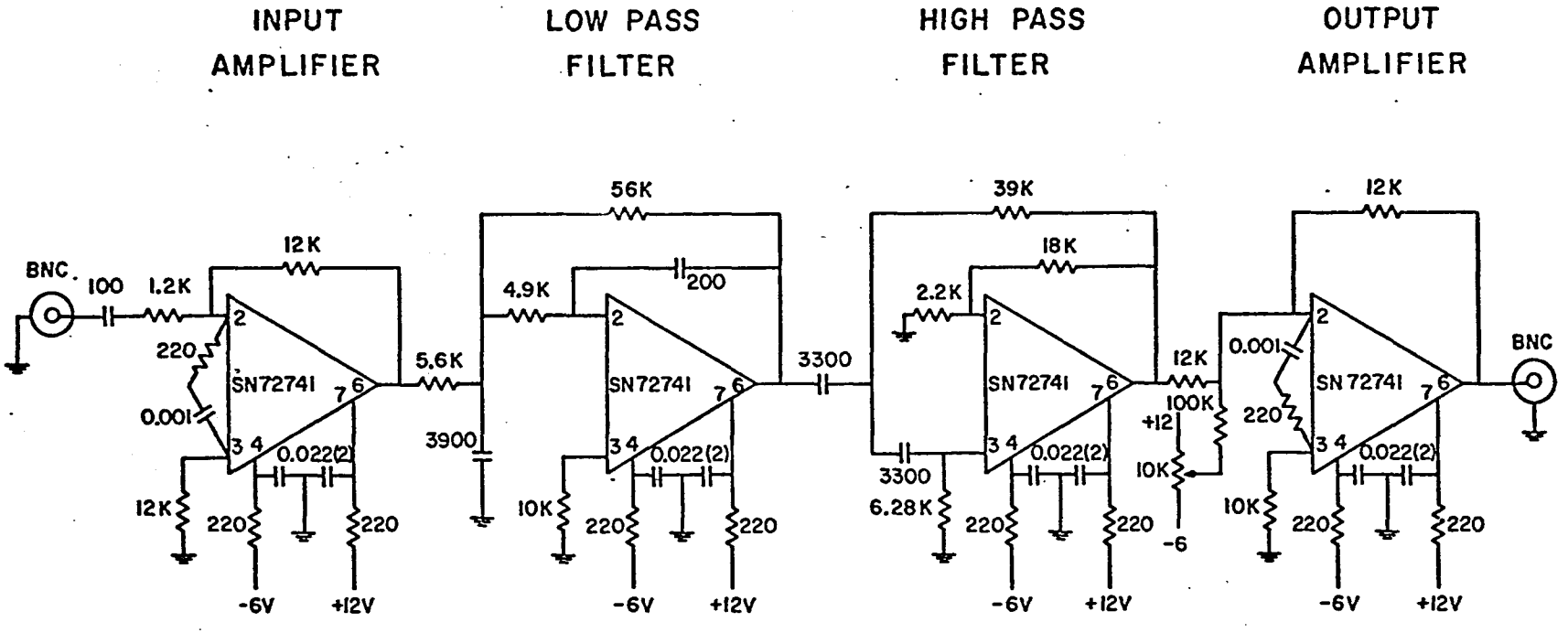
INPUT AMPLIFIER
LOW PASS FILTER
HIGH PASS FILTER
OUTPUT AMPLIFIER
BNC
100
1.2K
12K
220
0.001
SN72741
0.022(2)
12K
220
220
-6V
+12V
5.6K
3900
56K
4.9K
200
10K
39K
18K
2.2K
3300
6.28K
12K
100K
+12
10K
-6
0.001
BNC

Fig. 15

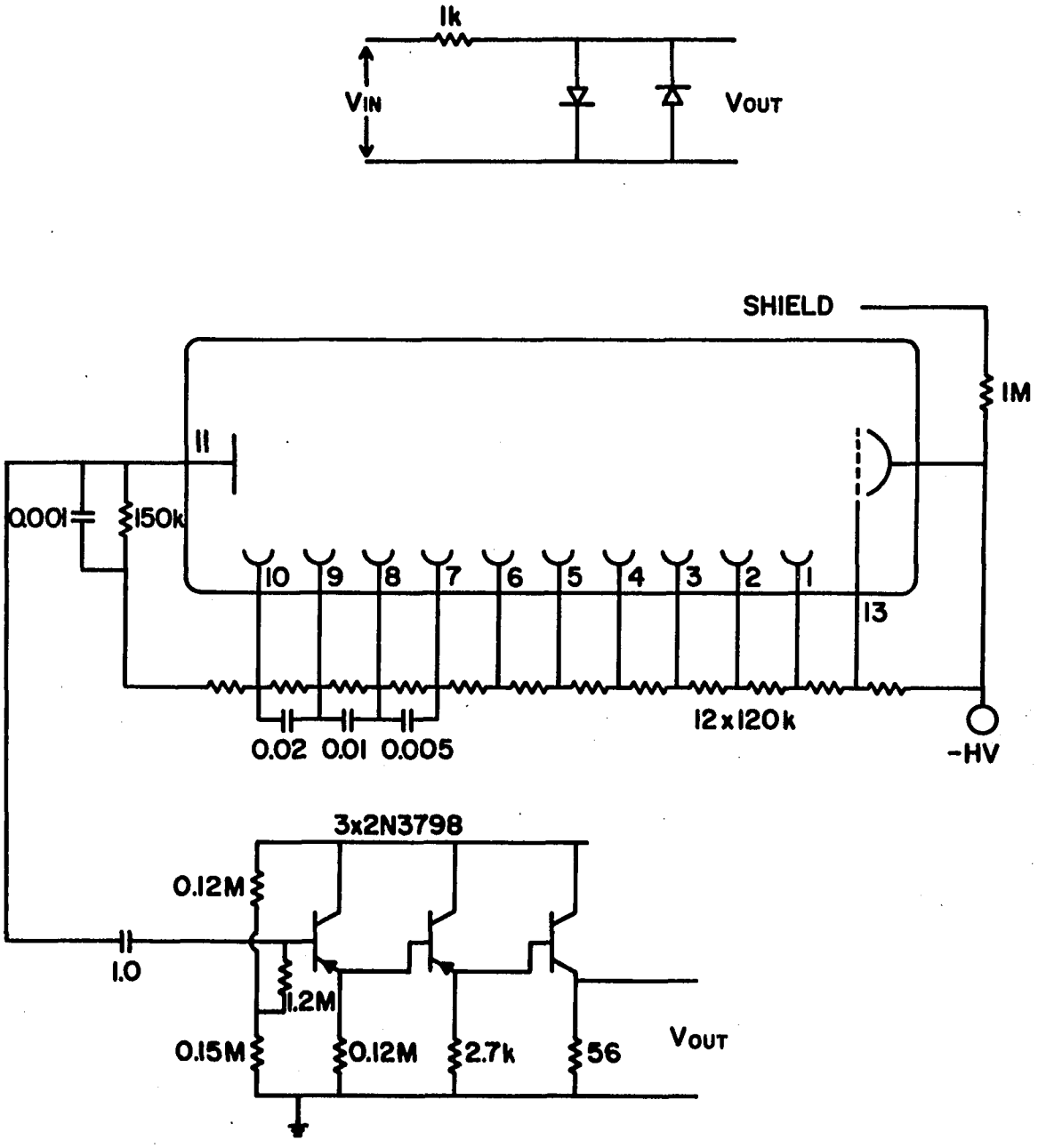
1k
VIN
VOUT
SHIELD
1M
11
0.001
150k
10
9
8
7
6
5
4
3
2
1
13
0.02
0.01
0.005
12x120k
-HV
3x2N3798
0.12M
1.0
1.2M
0.15M
0.12M
2.7k
56
VOUT

Fig. 16

REFERENCES

1. E. H. Wedemeyer, J. Fluid Mech. 20, 383 (1964).
2. G. Venezian, "Spin-Up of a Contained Fluid", in Topics in Ocean Engineering, ed. C. L. Bretschneider (Gulf Publishing Co., Houston, Texas, 1970) Vol. 1, p. 212.
3. G. Venezian, "Non-Linear Spin-Up", in Topics in Ocean Engineering, ed. C. L. Bretschneider (Gulf Publishing Co., Houston, Texas, 1971) Vol. 2, p. 87.
4. H. Goller and T. Ranov, J. Basic Engr. 90, 445 (1968).
5. A. R. McLeod, Phil. Mag. 44, 1 (1922).
6. H. P. Greenspan, The Theory of Rotating Fluids (Cambridge University Press, London, 1968) p. 165.
7. K. Stewartson, J. Fluid Mech. 3, 17 (1957).
8. M. H. Rogers and G. N. Lance, J. Fluid Mech. 7, 617 (1970).
9. G. K. Batchelor, An Introduction to Fluid Dynamics (Cambridge University Press, London, 1967) p. 204.
10. F. Durst, A. Melling and J. H. Whitelaw, J. Fluid Mech. 56, 143 (1972).
11. W. T. Mayo, J. Phys. E: Sci. Instrum. 3, 235 (1970).
12. J. F. Swindells, "The Viscosity of Water 0°C to 100°C", in Handbook of Chemistry and Physics, 49th Ed., ed. R. C. Weast (The Chemical Rubber Co., Cleveland, Ohio, 1968) p. F-36. The above table was calculated by

J. F. Swindells, and the calculations are derived from measurements at the National Bureau of Standards in viscometers calibrated with water at 20°C.

13. L. C. Caplan and R. Stern, Rev. Sci. Instrum. 42, 689 (1971).

14. Greenspan, op. cit., p. 4.

VITA

William Benton Watkins was born in Monroe, Louisiana, on July 6, 1946. He attended high school at West Monroe High School in West Monroe, Louisiana, and, upon graduation in 1964, enrolled in Louisiana State University. He received a Bachelor of Science degree in Physics in May of 1968. From September of 1968 through May of 1970, at which time he received a Master of Science degree in Physics, he was a graduate Teaching Assistant in the Department of Physics and Astronomy. From June of 1970 through December of 1972, he was a graduate Research Assistant in this department. From January 1973 through the present he has held a National Science Foundation Traineeship. He is presently a candidate for the Doctor of Philosophy degree in the Department of Physics and Astronomy.

EXAMINATION AND THESIS REPORT

Candidate: William Benton Watkins

Major Field: Physics

Title of Thesis: The Spin-Up from Rest of a Homogeneous, Viscous Fluid in a Right Cylindrical Container

Approved:

Robert D. Hussey
Major Professor and Chairman

Max Goodrich
Dean of the Graduate School

EXAMINING COMMITTEE:

Bruce M. Barker

Satya D. Verma

Edward Eganagi

Date of Examination:

April 30, 1973